Modeling blazar broadband emission with convolutional neural network

N. Sahakyan & D. Bégué

Content

- What are blazars ?
- Origin of emission: problems
- Developing convolutional neural network
- Results and applications

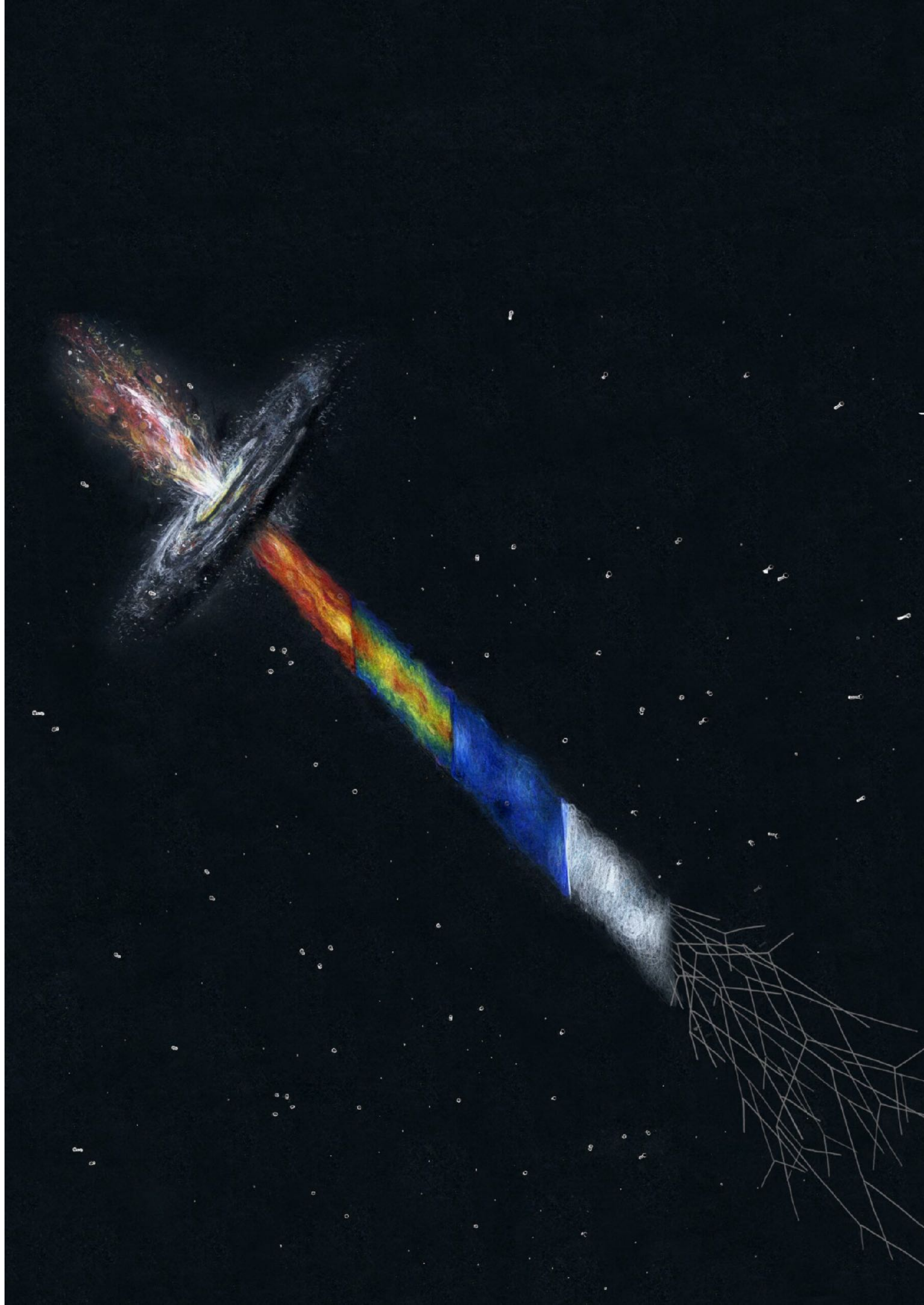

Jetted vs. non-jetted AGN

Non-jetted AGNs energy output is primarily radiation emitted from the accretion disk, as well as from the corona and potentially from a wind or outflow.

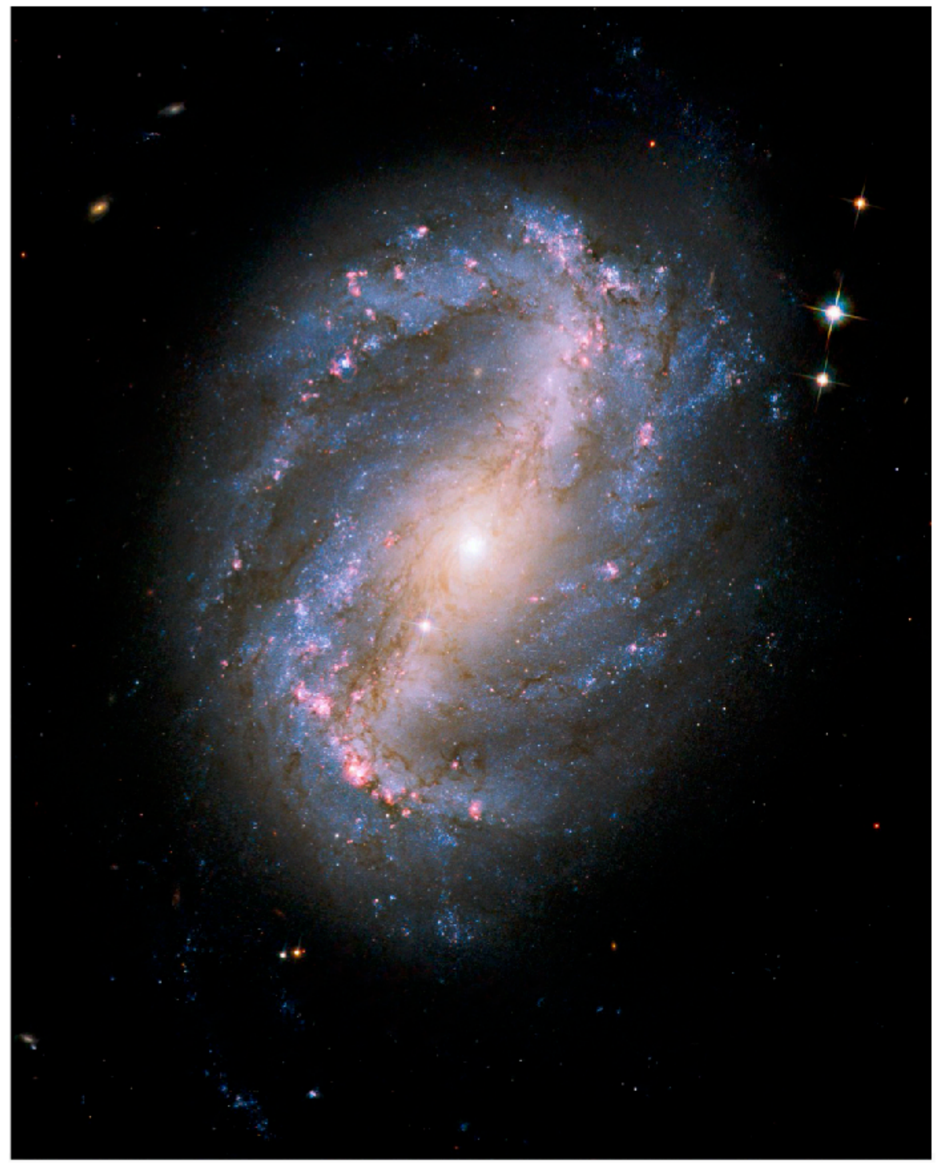

Jetted AGNs are a class of active galaxies that exhibit highly collimated, relativistic jets of plasma.

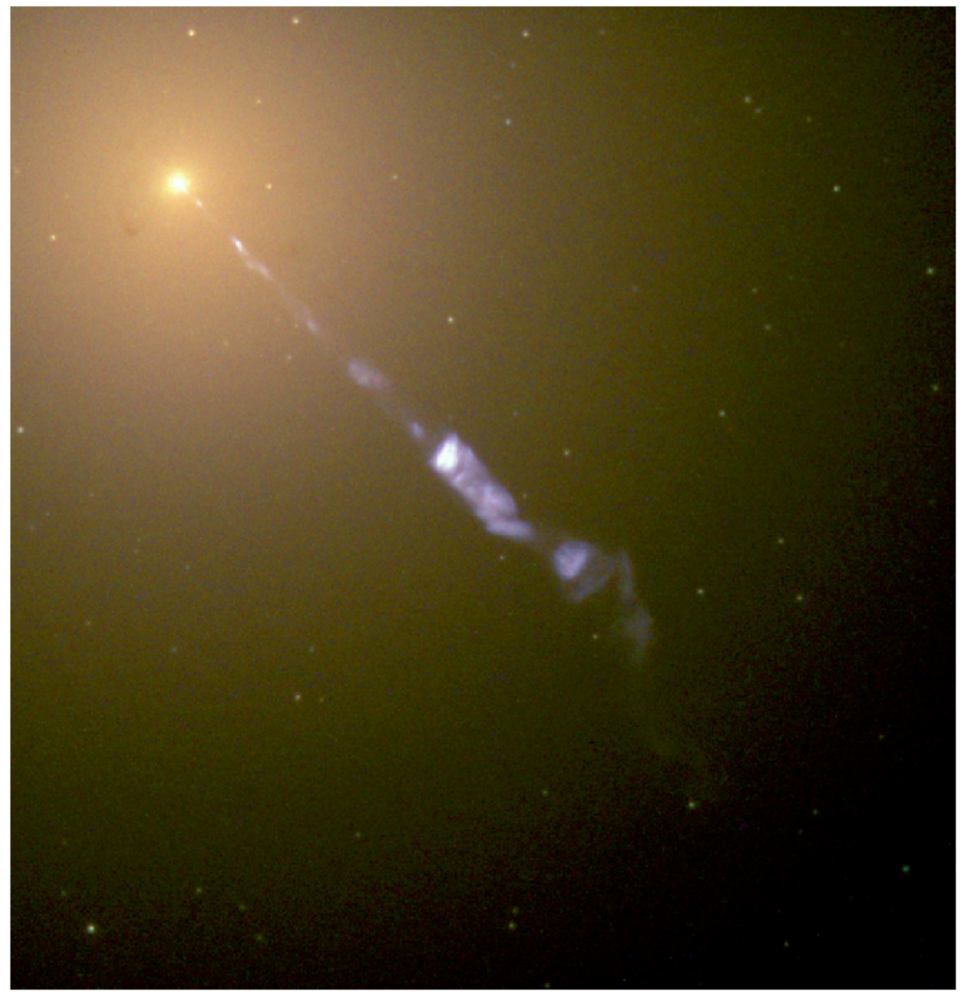

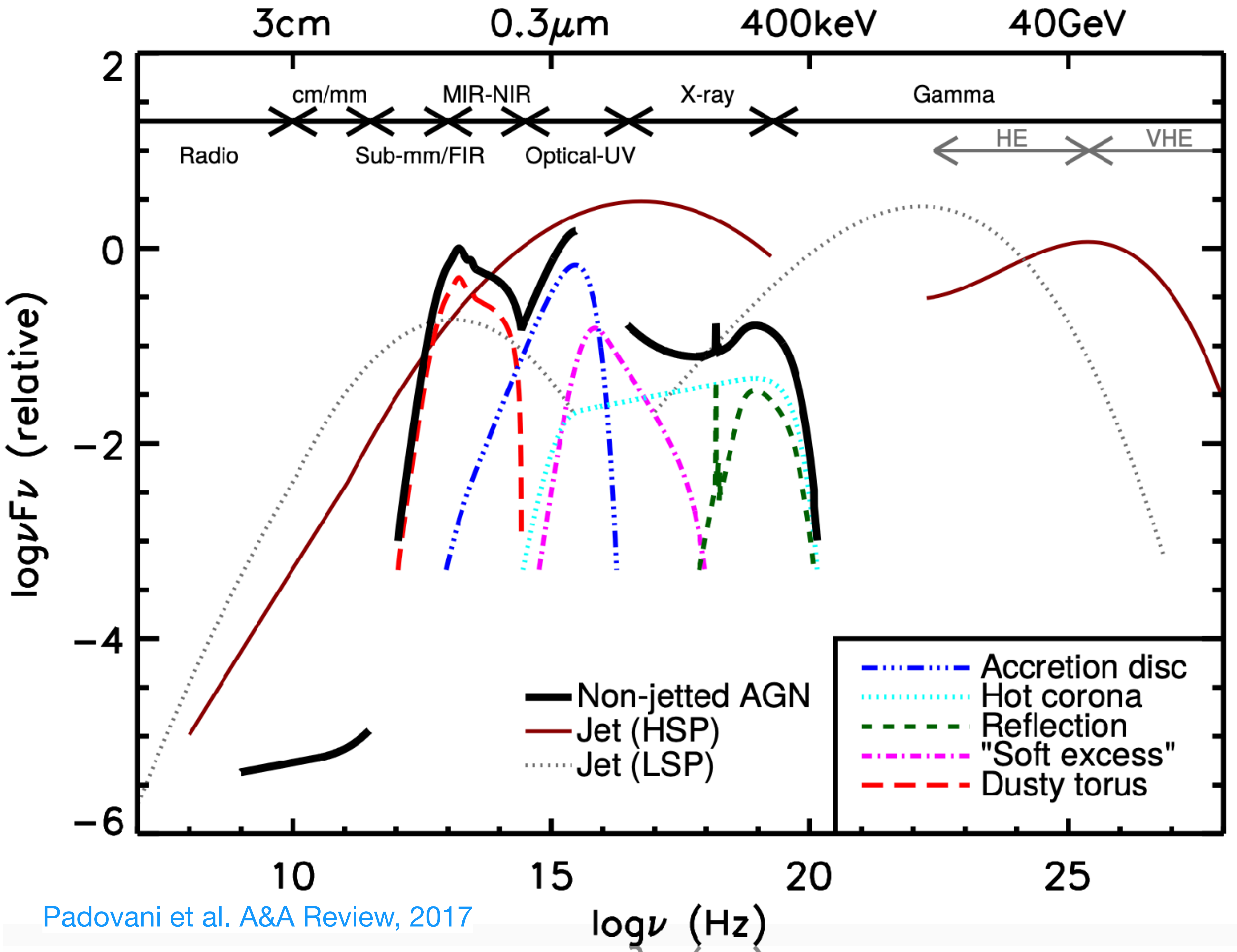

Padovani et al. A&A Review, 2017

Jetted vs. non-jetted AGN

Non-jetted AGNs energy output is primarily radiation emitted from the accretion disk, as well as from the corona and potentially from a wind or outflow.

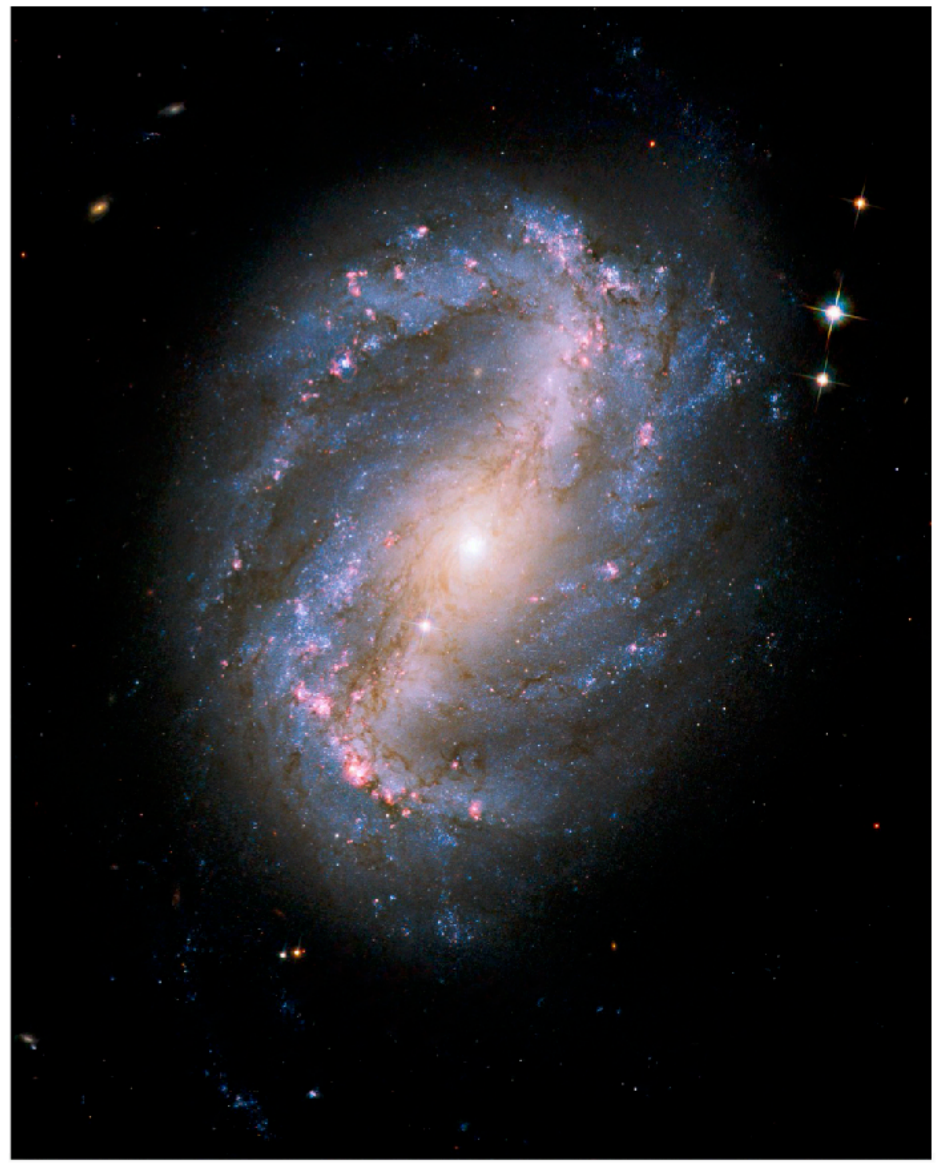

Jetted AGNs are a class of active galaxies that exhibit highly collimated, relativistic jets of plasma.

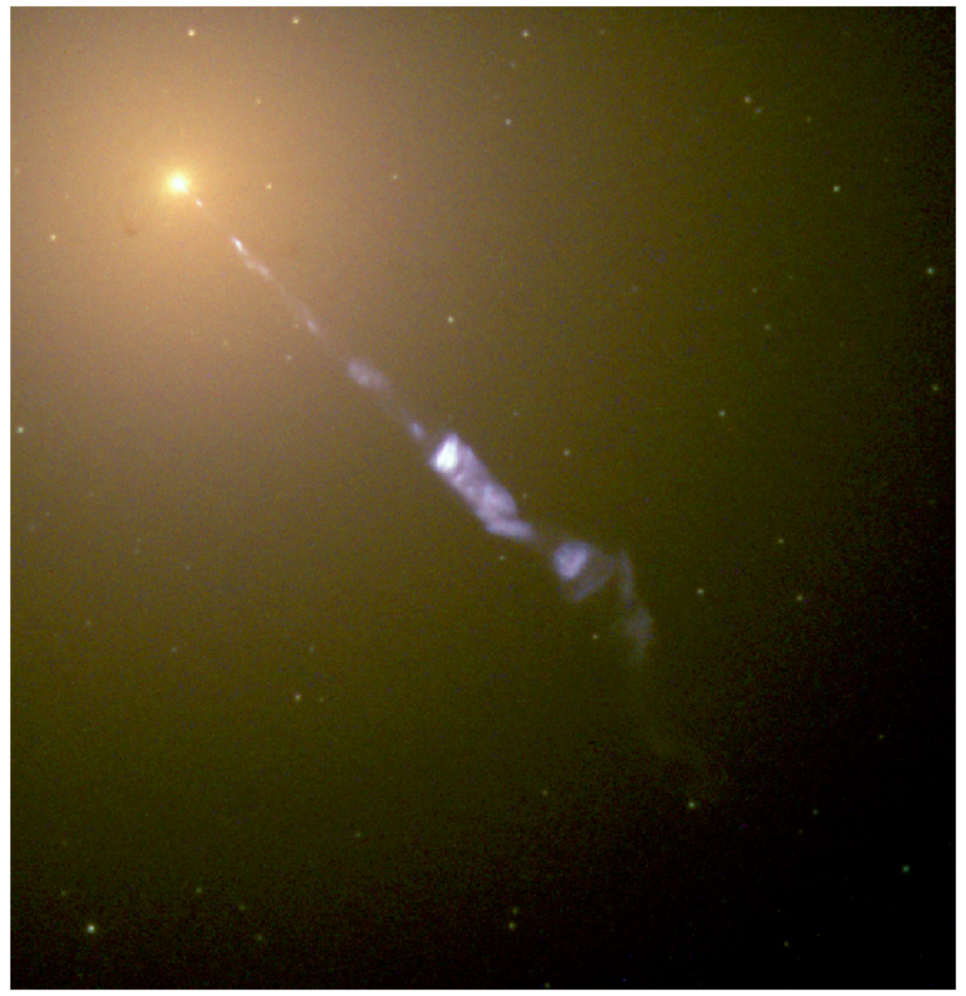

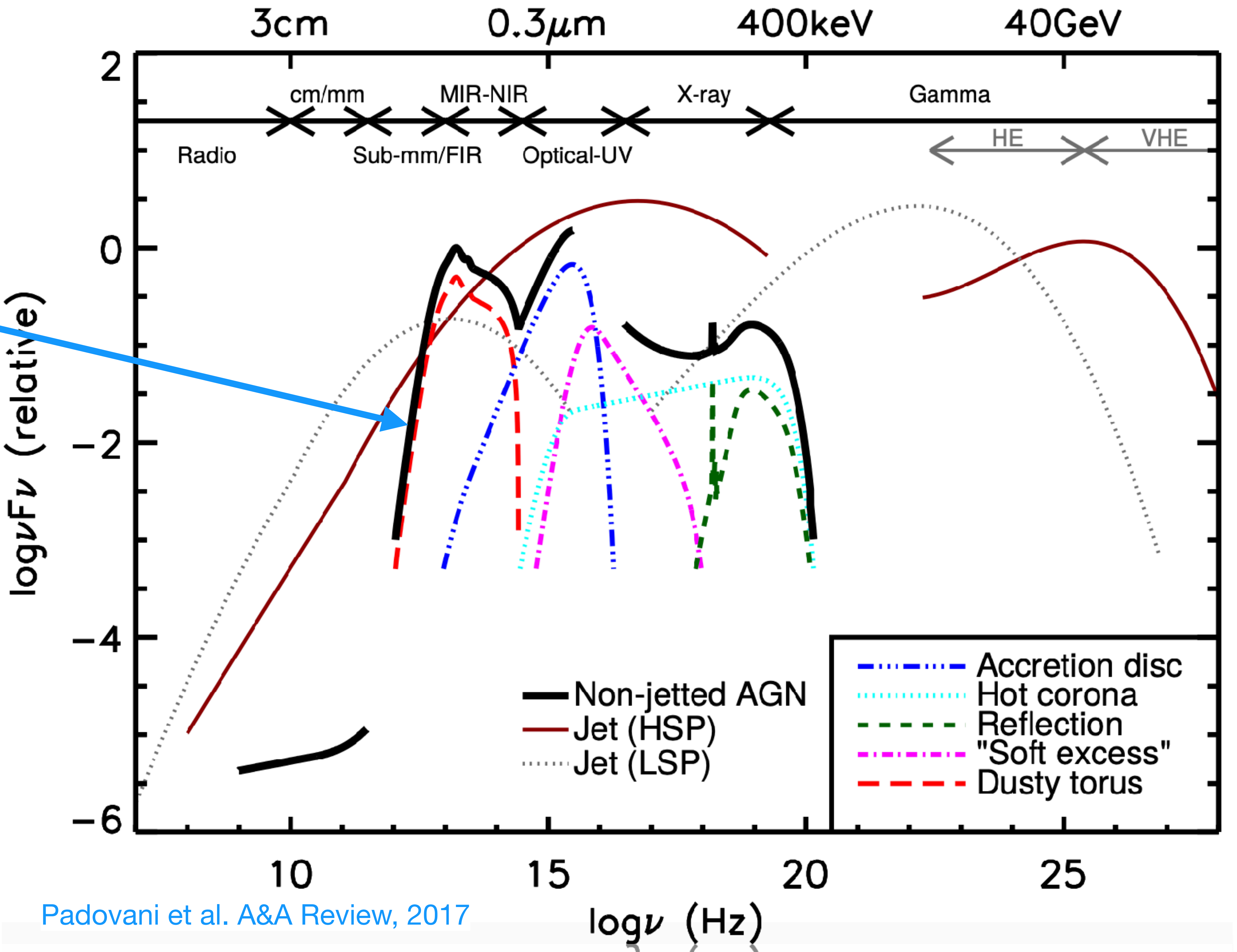

Padovani et al. A&A Review, 2017

Jetted vs. non-jetted AGN

Non-jetted AGNs energy output is primarily radiation emitted from the accretion disk, as well as from the corona and potentially from a wind or outflow.

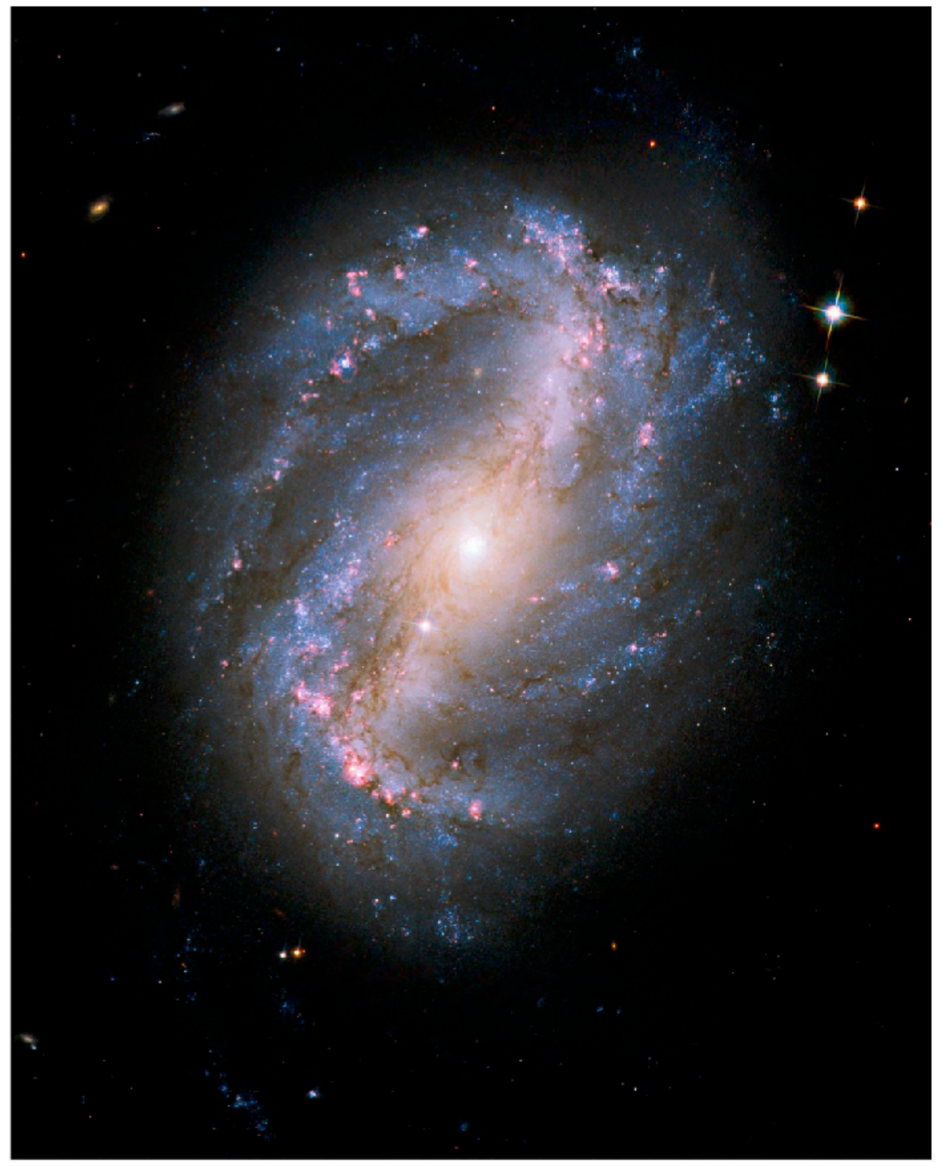

Jetted AGNs are a class of active galaxies that exhibit highly collimated, relativistic jets of plasma.

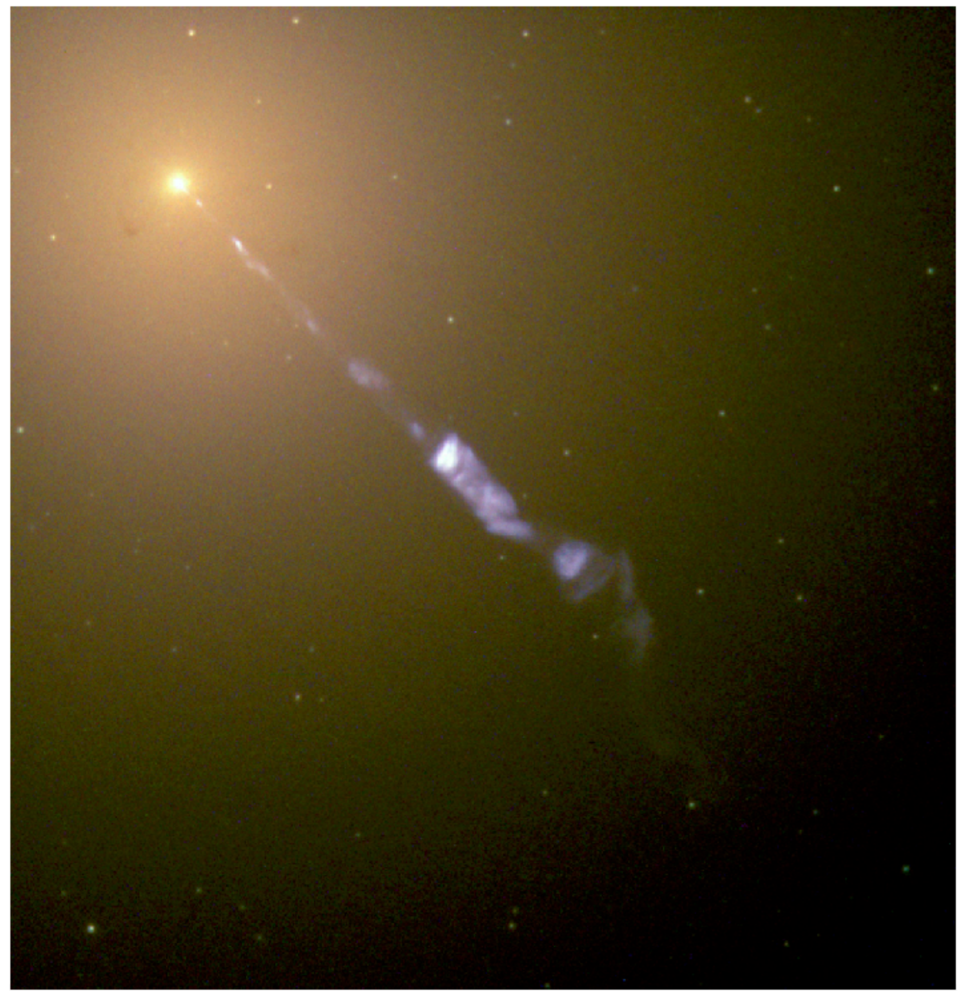

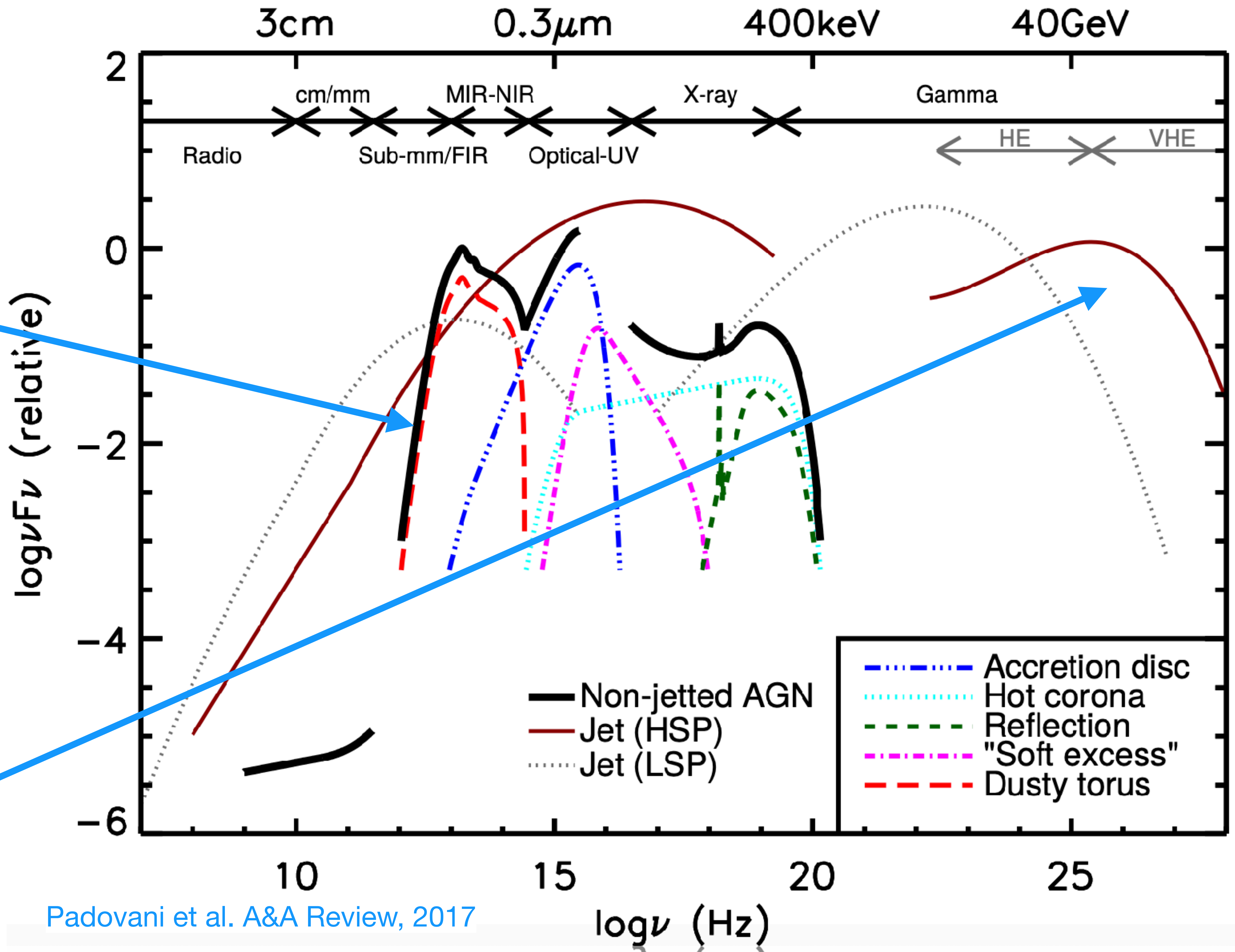

Padovani et al. A&A Review, 2017

Origin of the emission

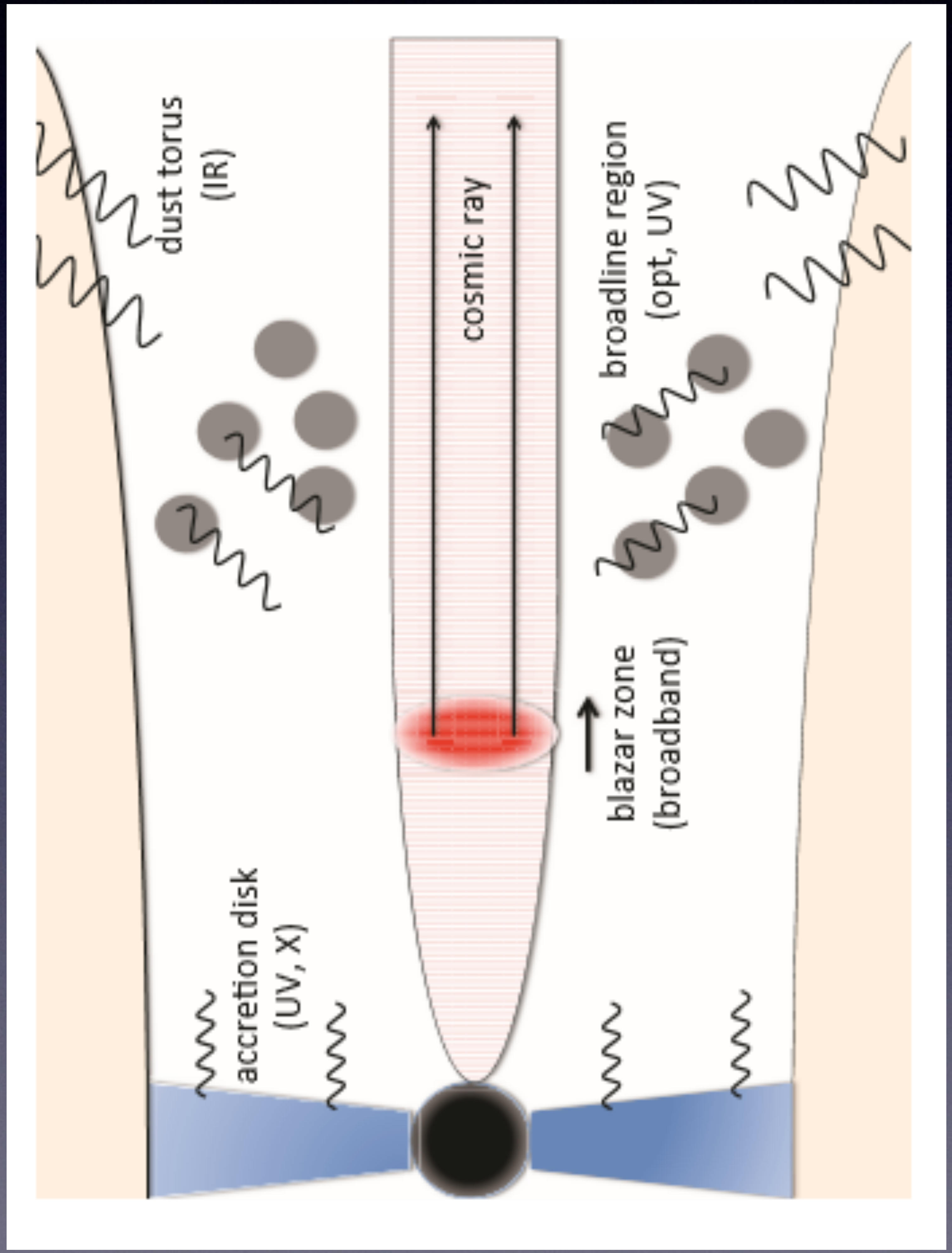

Origin of the emission

Injection or acceleration of electrons

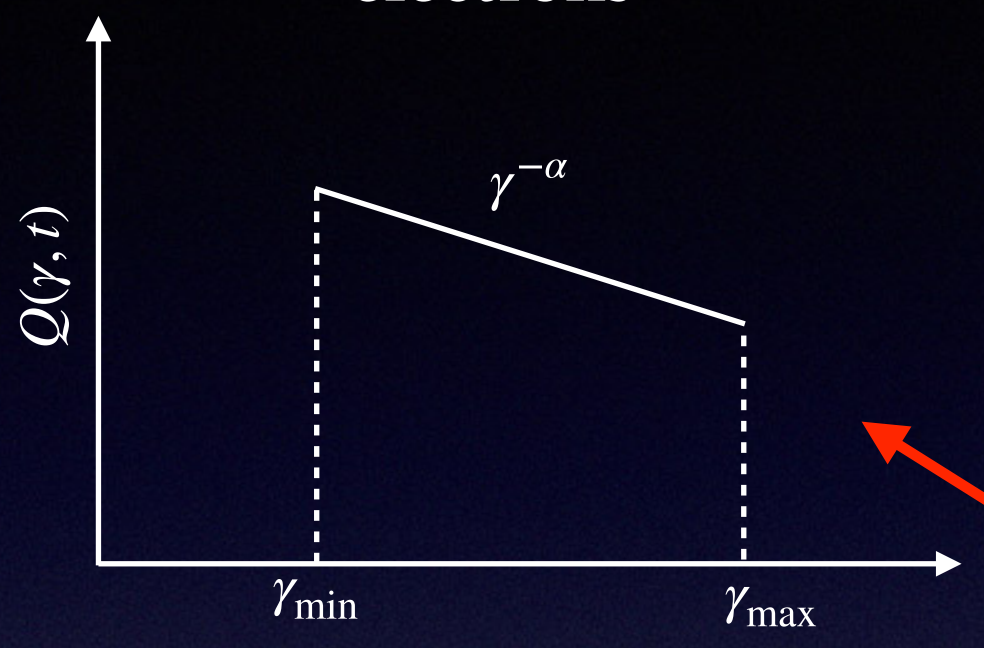

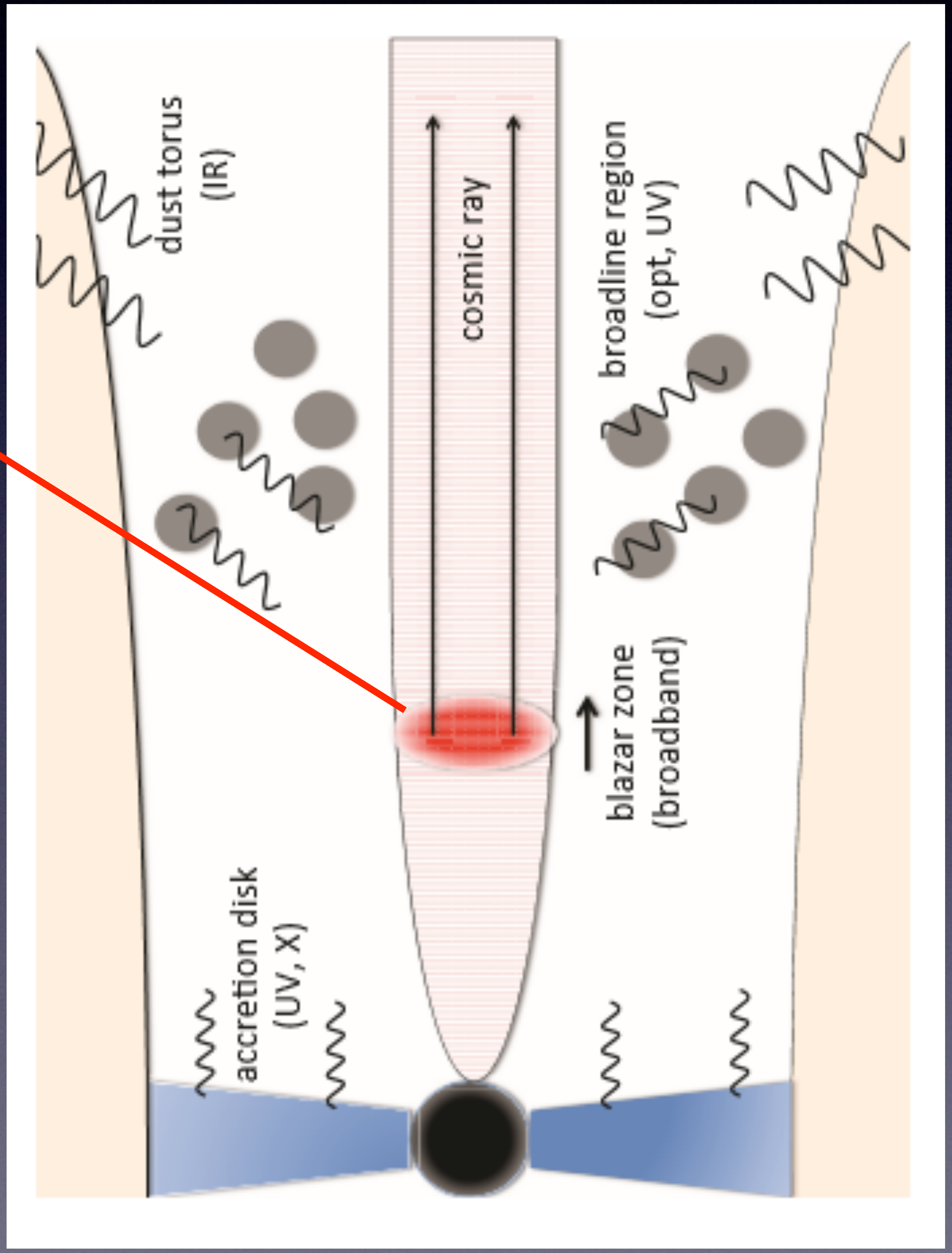

Origin of the emission

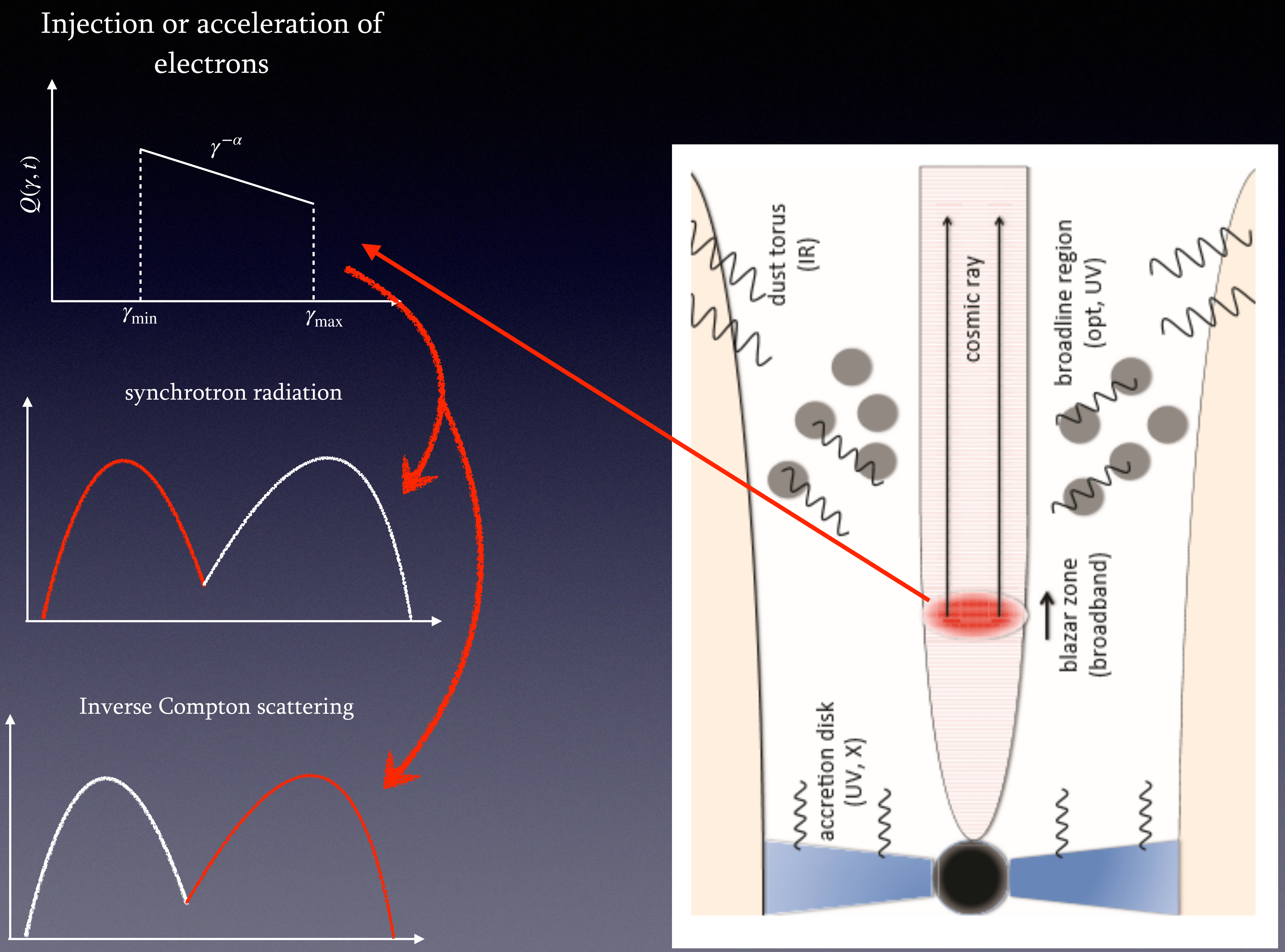

Origin of the emission

Injection or acceleration of electrons

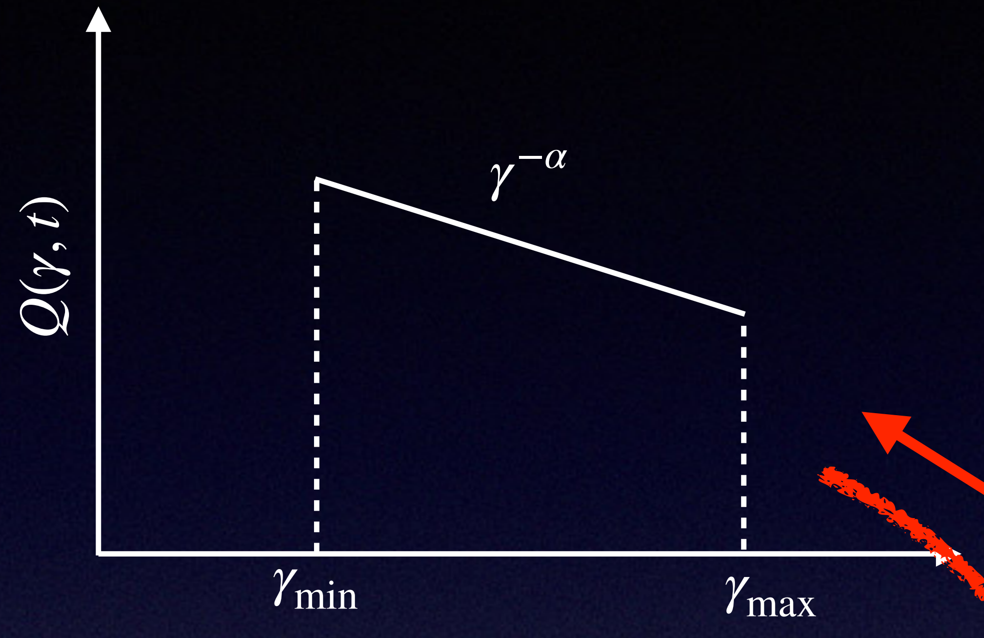

synchrotron radiation

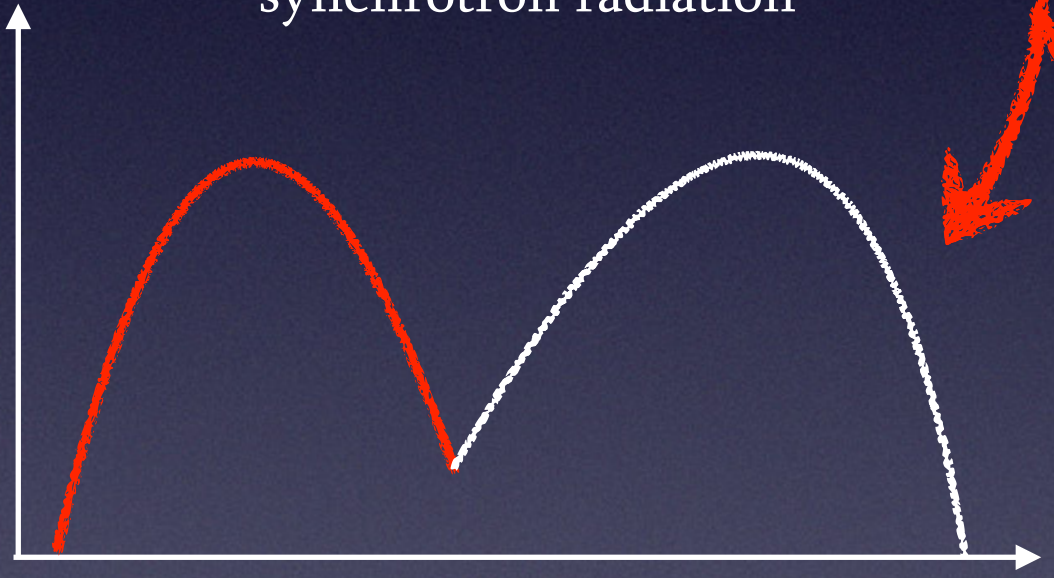

Inverse Compton scattering

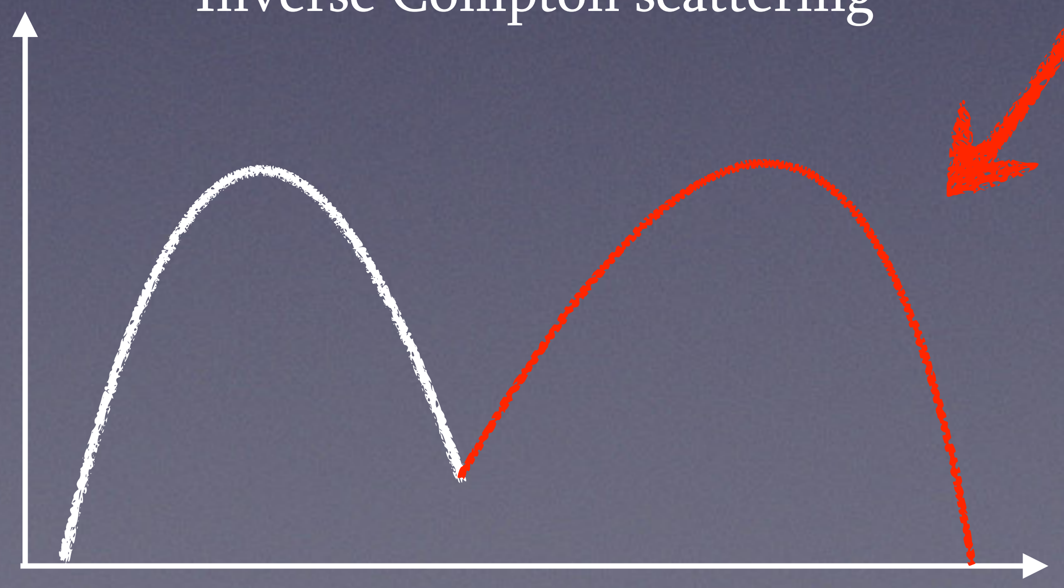

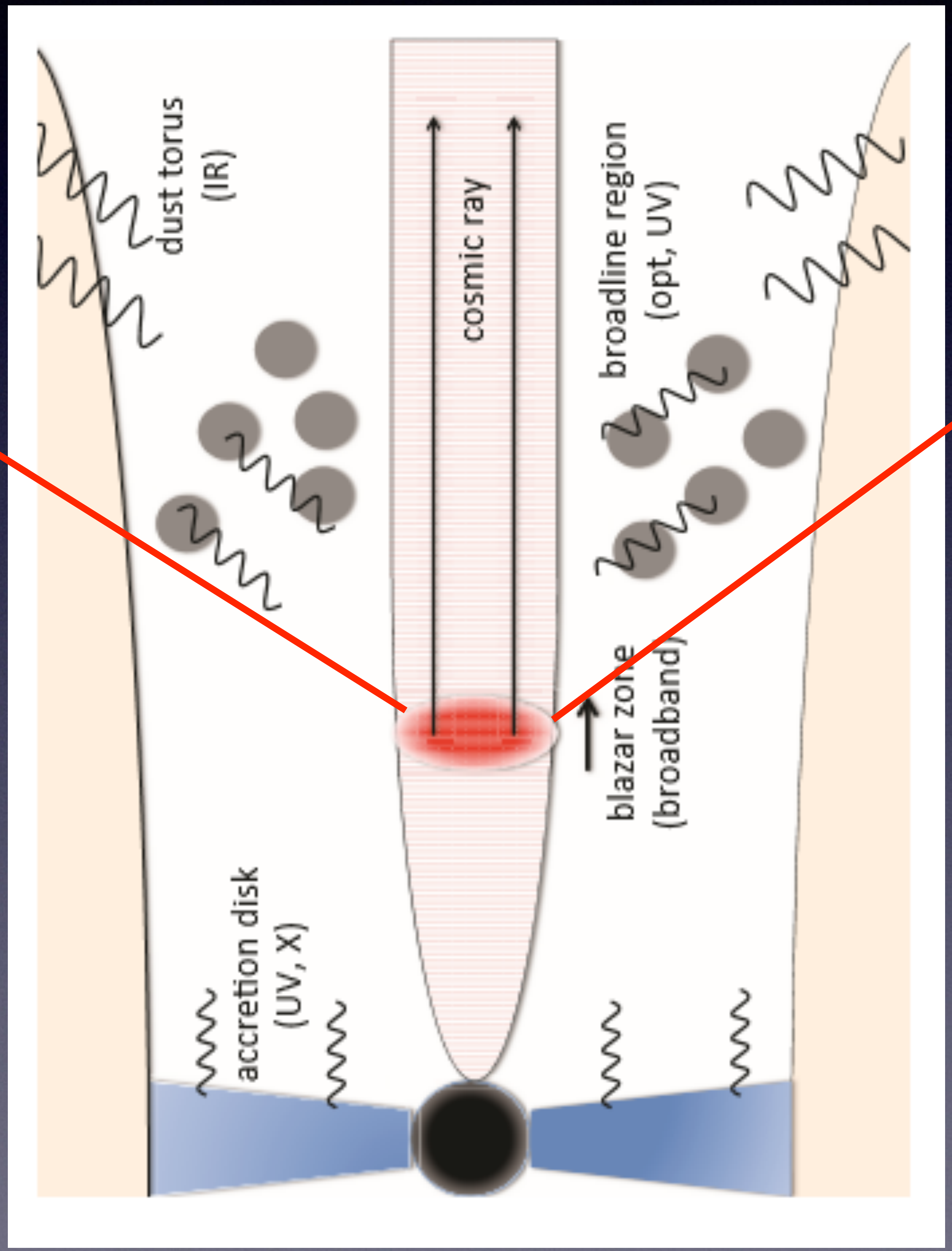

Injection or acceleration of protons

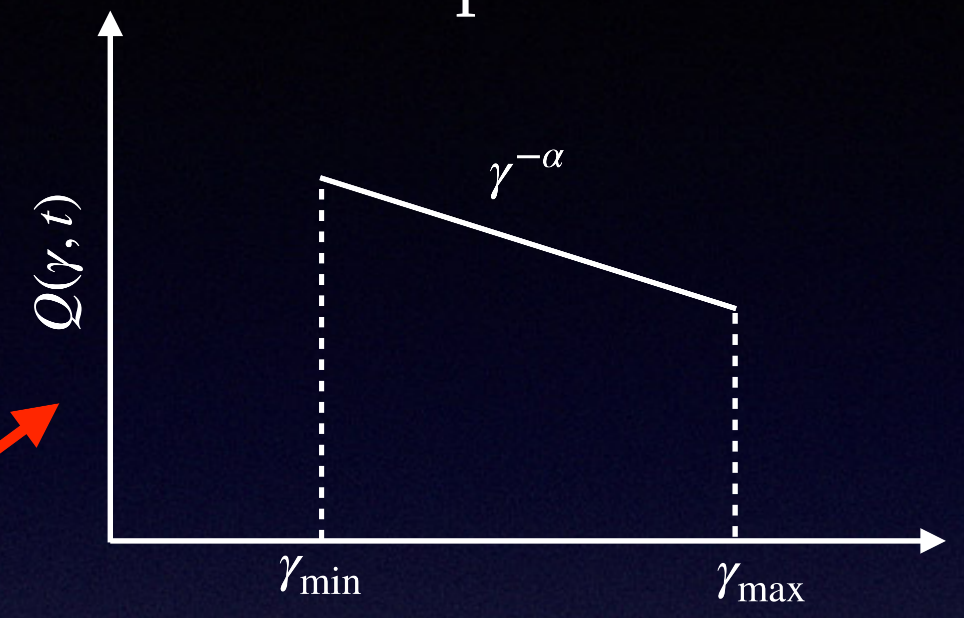

Origin of the emission

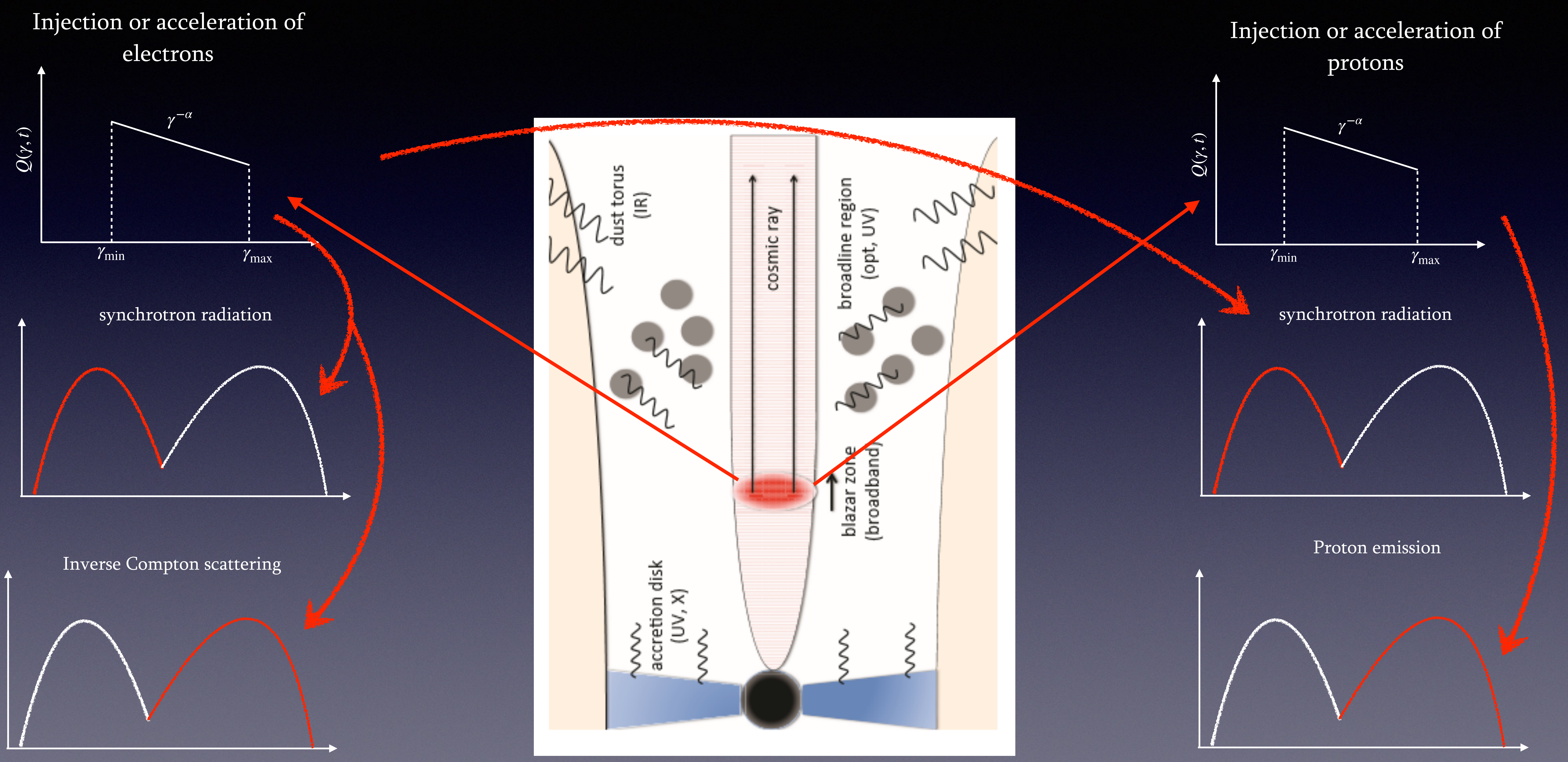

Evolution of the particle distribution

Gasparyan, Bégué, Sahakyan 2022

$$\begin{cases} \dfrac{\partial N_e}{\partial t}(\gamma) = \dfrac{N_e}{t_{\rm esc}} + \dfrac{\partial}{\partial \gamma}[(C_{\rm IC} N_\gamma + C_{\rm sync}) N_e \times] + Q_{\gamma\gamma \to e^+e^-}, \\ \dfrac{\partial N_\gamma}{\partial t}(x) = \dfrac{N_\gamma}{t_{\rm esc}} + Q_{\ \rm sync} + R_{\rm IC} N_\gamma - S_{\gamma\gamma \to e^+e^-}, \end{cases}$$

Evolution of the particle distribution

Gasparyan, Bégué, Sahakyan 2022

$$\begin{cases} \dfrac{\partial N_e}{\partial t}(\gamma) = \dfrac{N_e}{t_{\rm esc}} + \dfrac{\partial}{\partial \gamma}[(C_{\rm IC}N_\gamma + C_{\rm sync})N_e \times] + Q_{\gamma\gamma\to e^+e^-}, \\ \dfrac{\partial N_\gamma}{\partial t}(x) = \dfrac{N_\gamma}{t_{\rm esc}} + Q_{\rm\ sync} + R_{\rm IC}N_\gamma - S_{\gamma\gamma\to e^+e^-}, \end{cases}$$

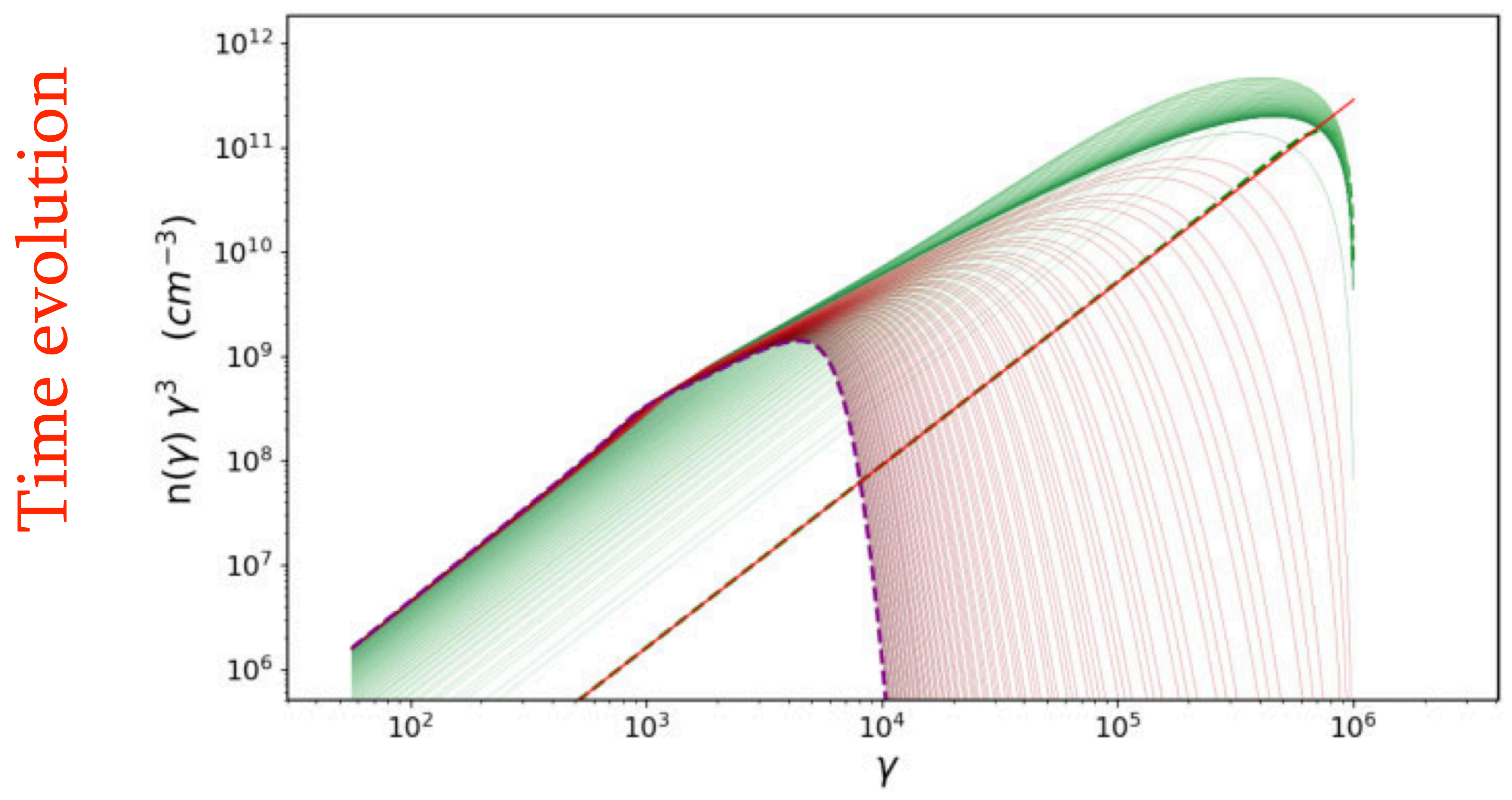

Evolution of the particle distribution

Gasparyan, Bégué, Sahakyan 2022

$$\begin{cases} \dfrac{\partial N_e}{\partial t}(\gamma) = \dfrac{N_e}{t_{\rm esc}} + \dfrac{\partial}{\partial \gamma}[(C_{\rm IC}N_\gamma + C_{\rm sync})N_e \times] + Q_{\gamma\gamma \to e^+e^-}, \\ \dfrac{\partial N_\gamma}{\partial t}(x) = \dfrac{N_\gamma}{t_{\rm esc}} + Q_{\rm \ sync} + R_{\rm IC}N_\gamma - S_{\gamma\gamma \to e^+e^-}, \end{cases}$$

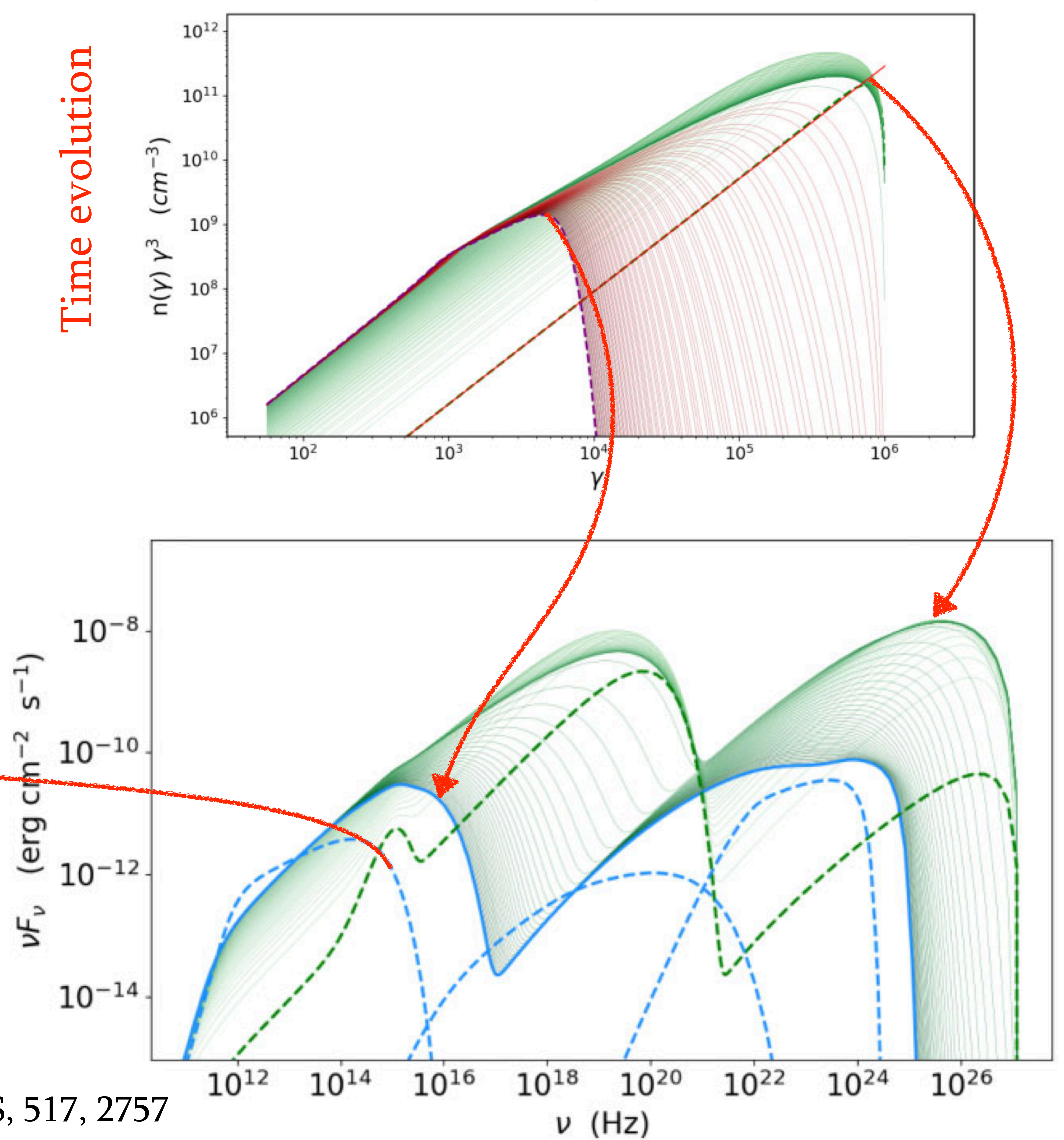

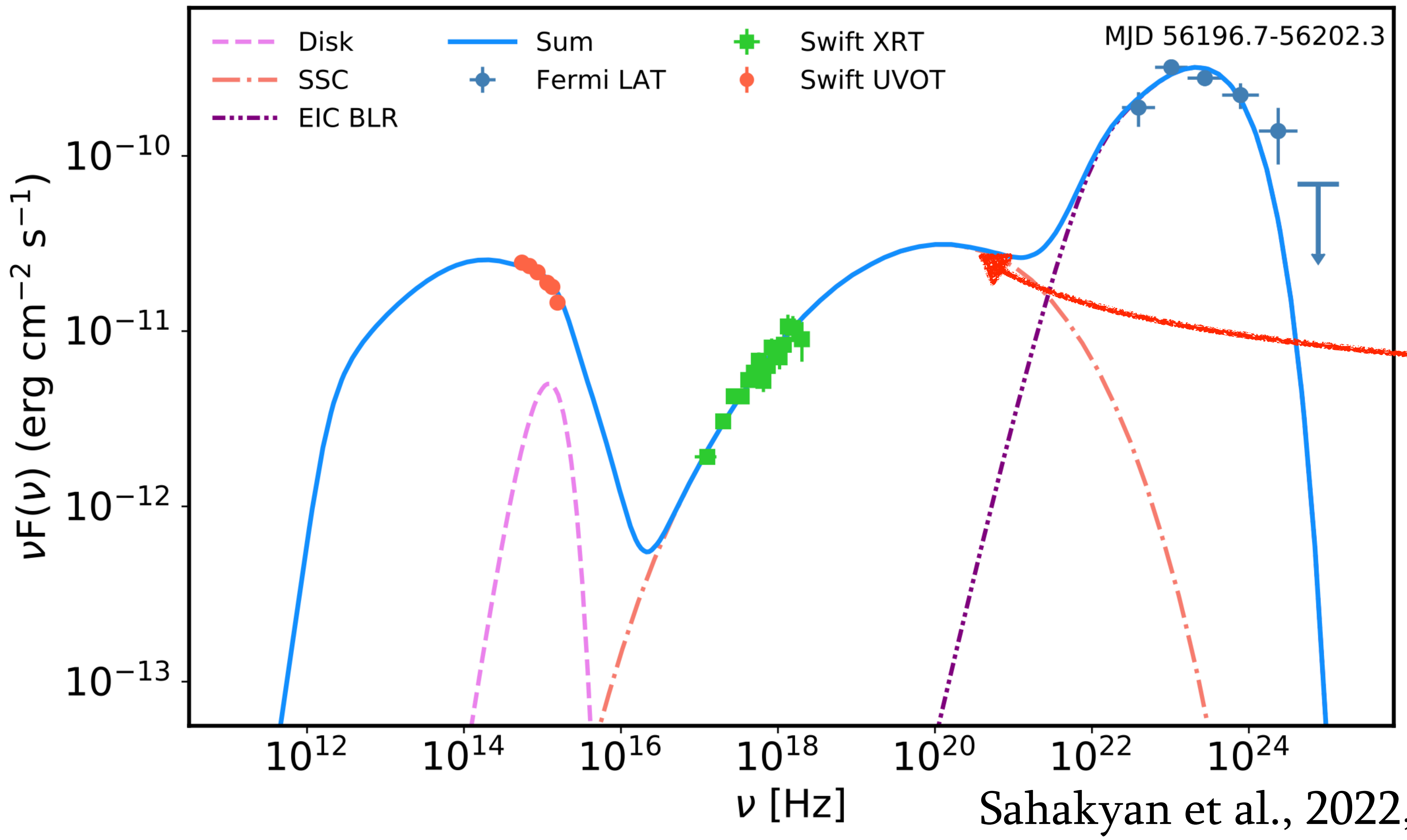

Sahakyan et al., 2022, MNRAS, 517, 2757

Parameter optimization

Parameter optimization

Put the model in a fitting engine.

- ➡ After waiting for a very long time, get an answer. If it works good, but if not, it is too expensive to redo it.
- ➡ Even though, limited to a couple of dataset.

Parameter optimization

Put the model in a fitting engine.

- After waiting for a very long time, get an answer. If it works good, but if not, it is too expensive to redo it.
- Even though, limited to a couple of dataset.

Table model

- Compute the model in wide parameter space
- Interpolate between sampled parameter sets

Parameter optimization

Put the model in a fitting engine.

- After waiting for a very long time, get an answer. If it works good, but if not, it is too expensive to redo it.
- Even though, limited to a couple of dataset.

Table model

- Compute the model in wide parameter space
- Interpolate between sampled parameter sets

For Bayesian fit $10^4 - 10^5$ times.

Average time for single spectrum calculations

SSC and EIC model: $\sim$ 30 sec (using 8 core)

✓ model computation time $\sim$ 3.5 – 35 days

hadronic model: $\sim$ 90 sec (using 8 core)

✓ model computation time $\sim$ 10.4 – 100 days

Parameter optimization

Put the model in a fitting engine.

- ➡ After waiting for a very long time, get an answer. If it works good, but if not, it is too expensive to redo it.
- ➡ Even though, limited to a couple of dataset.

Table model

- ➡ Compute the model in wide parameter space
- ➡ Interpolate between sampled parameter sets

<u>For Bayesian fit $10^4 - 10^5$ times.</u>

<u>Average time for single spectrum calculations</u>

SSC and EIC model: $\sim$ 30 sec (using 8 core)

✓ model computation time $\sim$ 3.5 – 35 days

hadronic model: $\sim$ 90 sec (using 8 core)

✓ model computation time $\sim$ 10.4 – 100 days

<u>Square parameter space, depending on the number of model parameters</u>

SSC (7 free parameters): $10^6 - 10^7$ times.

EIC (11 free parameters): $> 10^7$ times.

files with size > 250 Gb

Change the model ?

Change the model ?

$\boxed{\text{Make the model faster}}$ numerical code $\xrightarrow{\text{approximations}}$ semi-analytical + numerical code

factor of ~ 2 gain but the model needs to be computed EVERY time

Change the model ?

Make the model faster

numerical code $\xrightarrow{\text{approximations}}$ semi-analytical + numerical code

factor of ~ 2 gain but the model needs to be computed EVERY time

Machine learning:

✓ Model will be computed once and can be used with different datasets.

✓ It does not require a square parameter space, which makes it less computationally expensive. It allows for model failure which can be removed from the training

Change the model ?

Make the model faster

numerical code $\xrightarrow{\text{approximations}}$ semi-analytical + numerical code

factor of ~ 2 gain but the model needs to be computed EVERY time

Machine learning:

✓ Model will be computed once and can be used with different datasets.

✓ It does not require a square parameter space, which makes it less computationally expensive. It allows for model failure which can be removed from the training

Latin hypercube sampling method is a widely popular technique in the creation of surrogate models as it presents several advantages. First, it allows to specify the number of simulations to be computed. As a byproduct, this method does not require to specify parameter spacing. Second, it ensures uniform sampling across all parameters. Lastly, it avoids the regular sampling of parameters, which is typical in grid scan techniques.

Workflow of the method

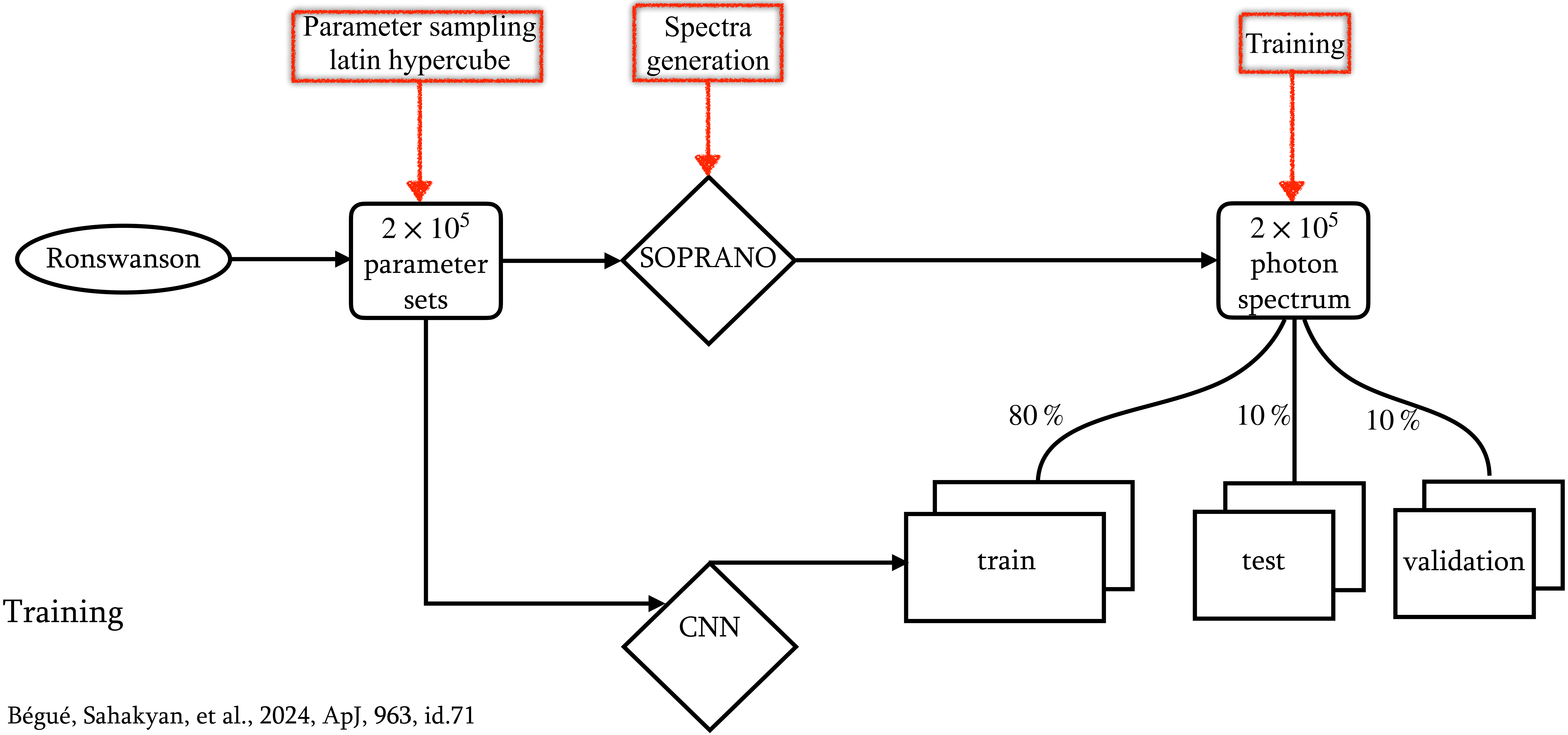

Training

Bégué, Sahakyan, et al., 2024, ApJ, 963, id.71

Parameter Sampling

This large range of parameters guarantees that any blazar SED can be reproduced.

synchrotron self Compton

Parameter	Units	Symbol	Minimum	Maximum	Type of distribution
Doppler boost	-	δ	3	50	Linear
Blob radius	cm	R	10^{15}	10^{18}	Logarithmic
Minimum electron injection Lorentz factor	-	$\gamma_{\rm min}$	$10^{1.5}$	10^{5}	Logarithmic
Maximum electron injection Lorentz factor	-	$\gamma_{\rm max}$	10^{2}	10^{8}	Logarithmic
Injection index	-	p	1.8	5	Linear
Electron luminosity	erg.s^{-1}	L_e	10^{42}	10^{48}	Logarithmic
Magnetic field	G	B	10^{-3}	10^{2}	Logarithmic

Bégué, Sahakyan, et al., 2024, ApJ, 963, id.71

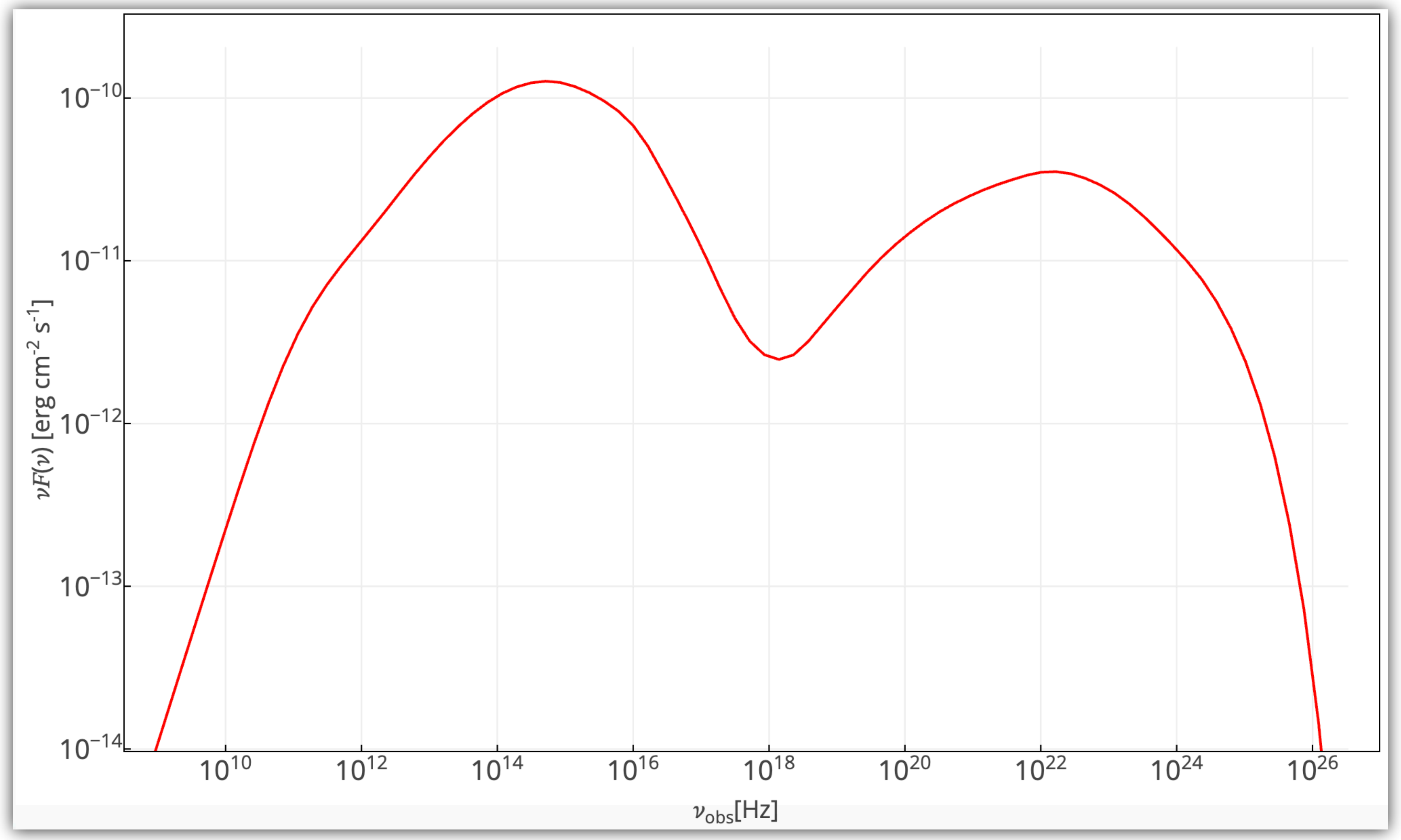

External inverse Compton

Parameters	Units	Symbol	Minimum	Maximum	Type of distribution
Doppler boost	-	δ	3	50	Linear
Blob radius	cm	R	10^{15}	10^{18}	Logarithmic
Minimum electron Lorentz factor	-	$\gamma_{\rm min}$	$10^{1.5}$	10^{5}	Logarithmic
Maximum electron Lorentz factor	-	$\gamma_{\rm max}$	10^{2}	10^{6}	Logarithmic
Injection index	-	p	1.8	5	Linear
Electron luminosity	erg.s^{-1}	L_e	10^{42}	10^{48}	Logarithmic
Magnetic field	G	B	10^{-3}	$10^{2.5}$	Logarithmic
Black hole mass	$M_\odot$	$M_{\rm BH}$	10^{7}	10^{10}	Logarithmic
Disk luminosity	erg.s^{-1}	L_d	$10^{43.5}$	$10^{47.5}$	Logarithmic
BLR frequency	Hz	$\nu_{\rm BLR}$	$10^{14.5}$	10^{16}	Logarithmic
DT frequency	Hz	$\nu_{\rm DT}$	$10^{12.5}$	10^{14}	Logarithmic

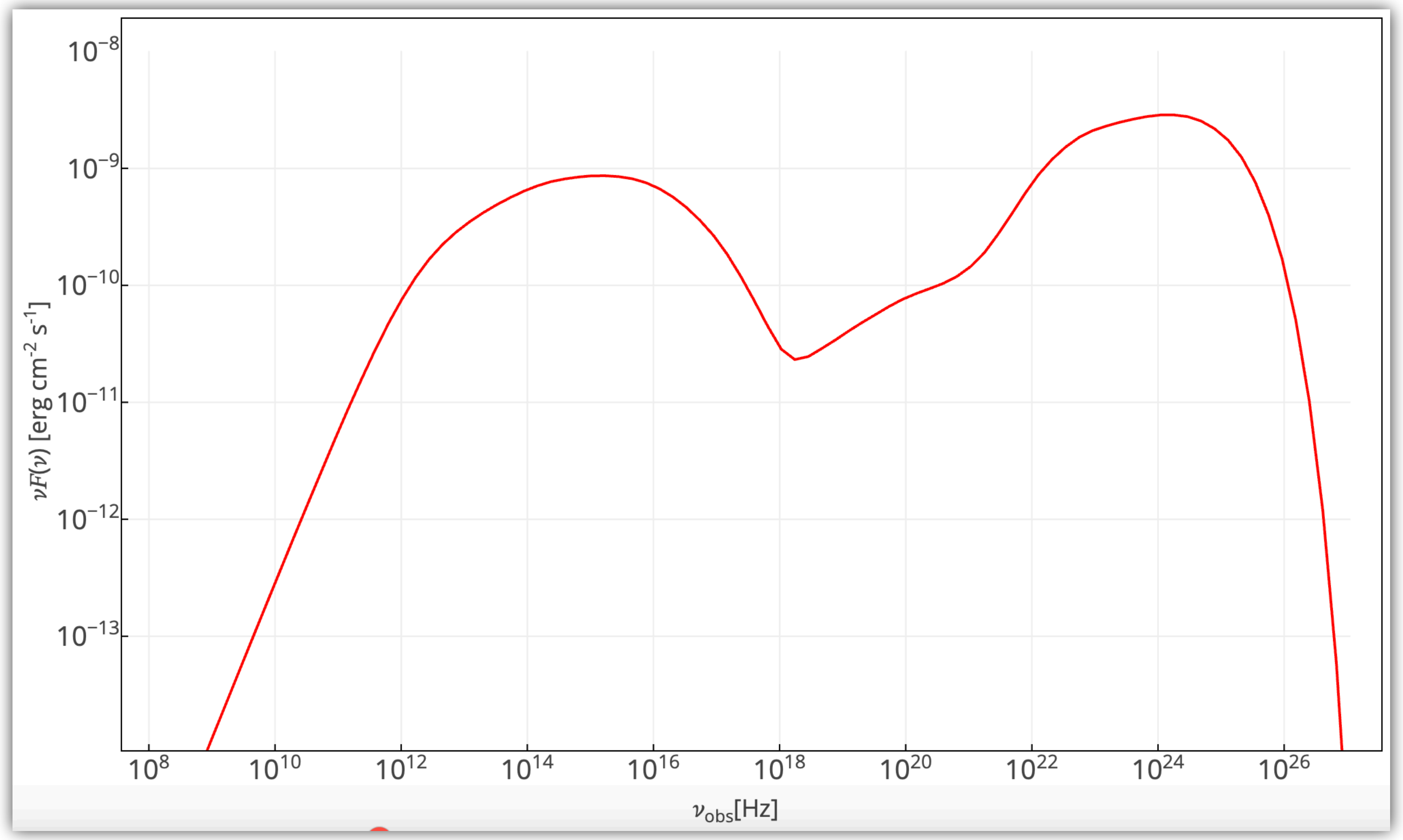

Sahakyan, Bégué, et al., 2024, arXiv:2402.07495

Spectrum generation: Time dependent approach

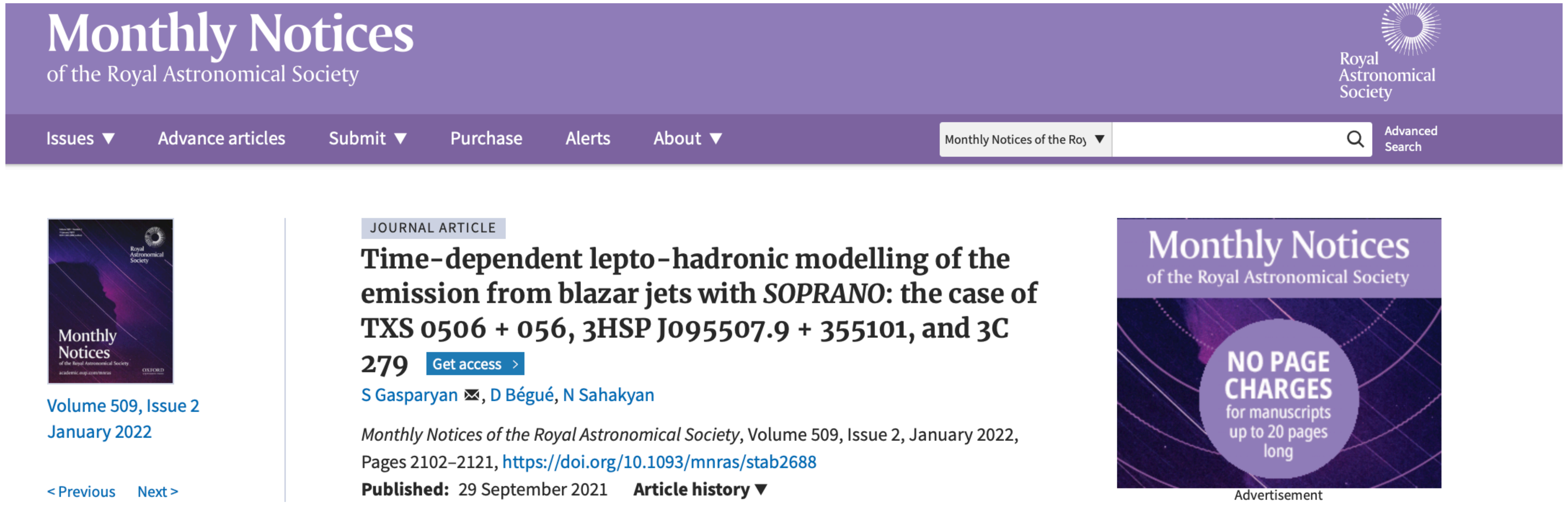
Monthly Notices of the Royal Astronomical Society

Issues ▼ Advance articles Submit ▼ Purchase Alerts About ▼

Volume 509, Issue 2
January 2022

< Previous Next >

JOURNAL ARTICLE

Time-dependent lepto-hadronic modelling of the emission from blazar jets with *SOPRANO*: the case of TXS 0506 + 056, 3HSP J095507.9 + 355101, and 3C 279

S Gasparyan, D Bégué, N Sahakyan

Monthly Notices of the Royal Astronomical Society, Volume 509, Issue 2, January 2022, Pages 2102–2121, https://doi.org/10.1093/mnras/stab2688

Published: 29 September 2021 **Article history** ▼

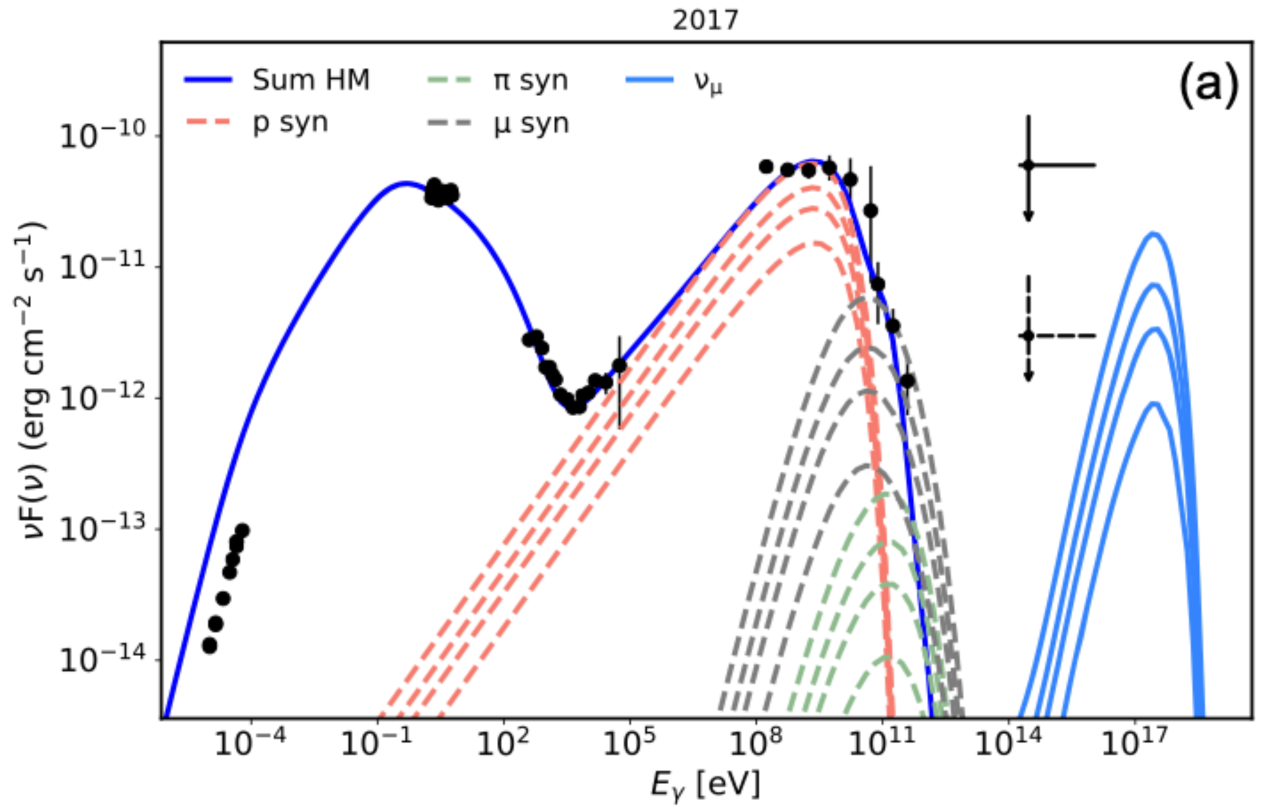

Gasparyan, Bégué, Sahakyan 2022

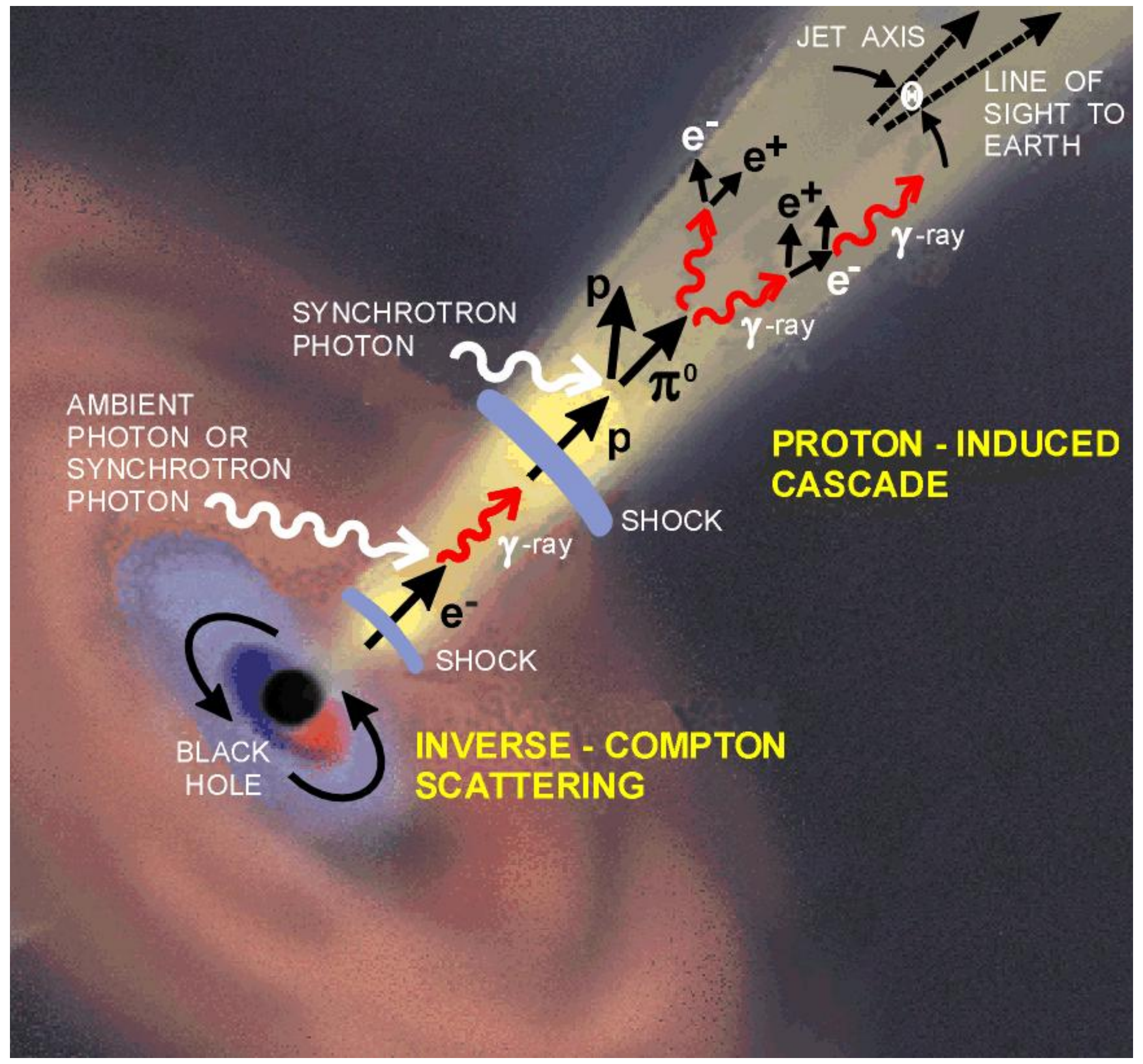

$$\frac{\partial N_p}{\partial t} = C_{p\gamma\rightarrow p\pi} + C_{p\gamma\rightarrow e^+e^-} + C_{\rm synch} - S_{\gamma p\rightarrow n\pi} + Q_{\gamma n\rightarrow p\pi}$$

$$\frac{\partial N_\mu}{\partial t} = Q_{\pi_\pm} - S_\mu + C_{\rm synch}$$

$$\frac{\partial N_n}{\partial t} = -S_{n\gamma\rightarrow p\pi} + Q_{p\gamma\rightarrow n\pi} + C_{n\gamma\rightarrow n\pi}$$

$$\frac{\partial N_{\nu,\zeta}}{\partial t} = Q_{\pi_\pm} + Q_\mu$$

$$\frac{\partial N_{\pi_\pm}}{\partial t} = Q_{p\gamma\rightarrow\pi} + Q_{n\gamma\rightarrow\pi} - S_\pi + C_{\rm synch}$$

$$\frac{\partial N_{e^\pm}}{\partial t} = Q_\mu + Q_{p\gamma\rightarrow e^+e^-} + Q_{\gamma\gamma\rightarrow e^+e^-}C_{\rm IC} + C_{\rm synch}$$

Q: sink term S: source term C: cooling term

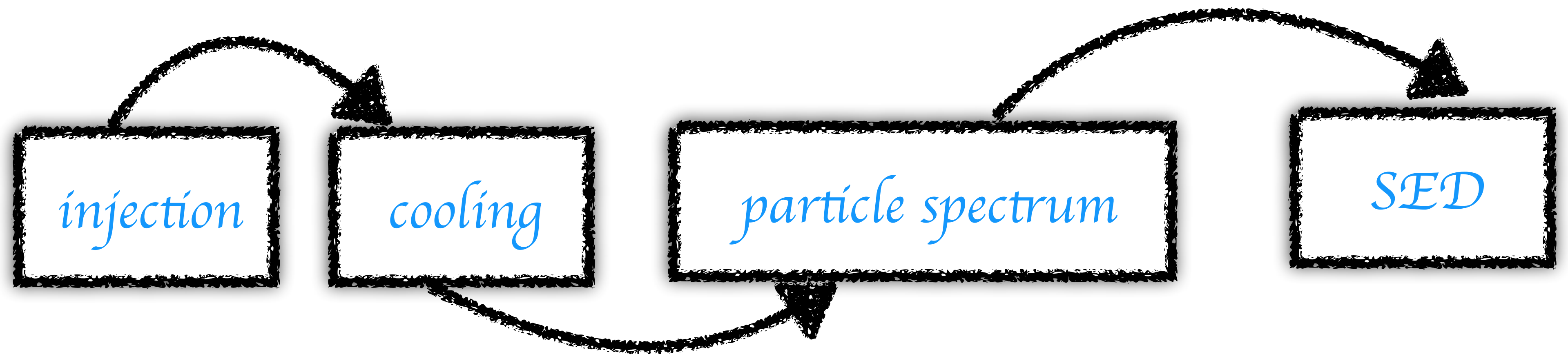

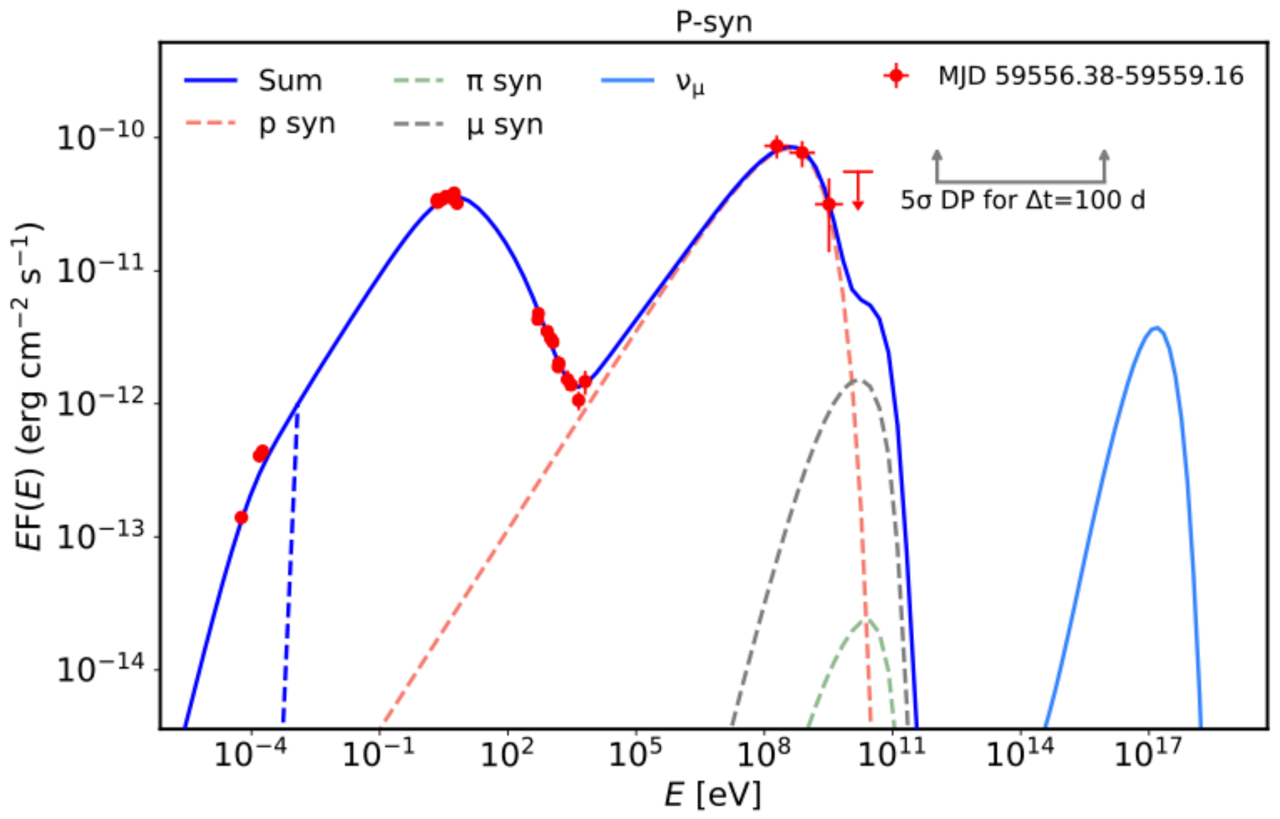

Sahakyan et al., 2023

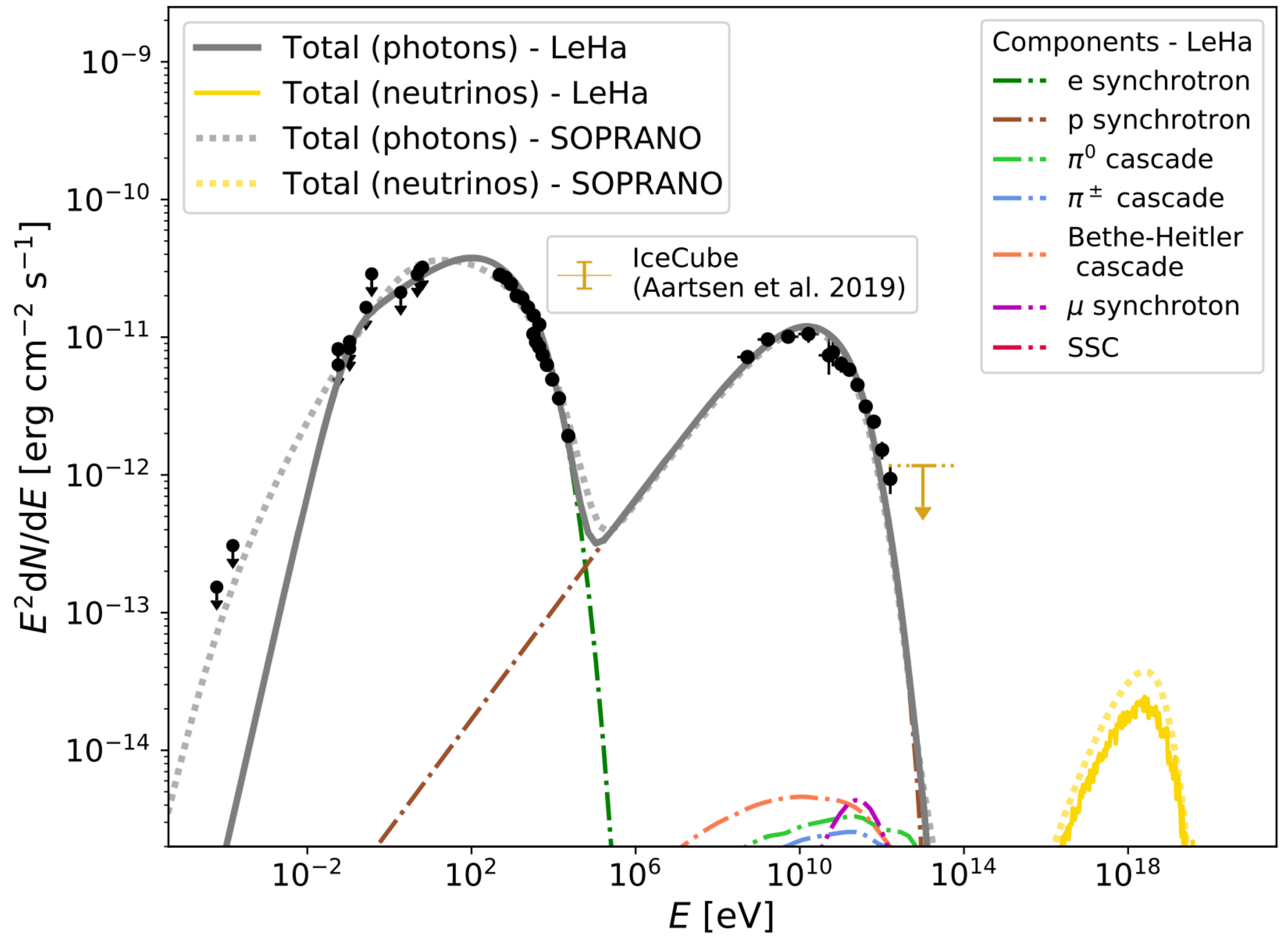

Abe et al., 2023

Computation

synchrotron self Compton

2×10^5 parameter sets → SOPRANO →

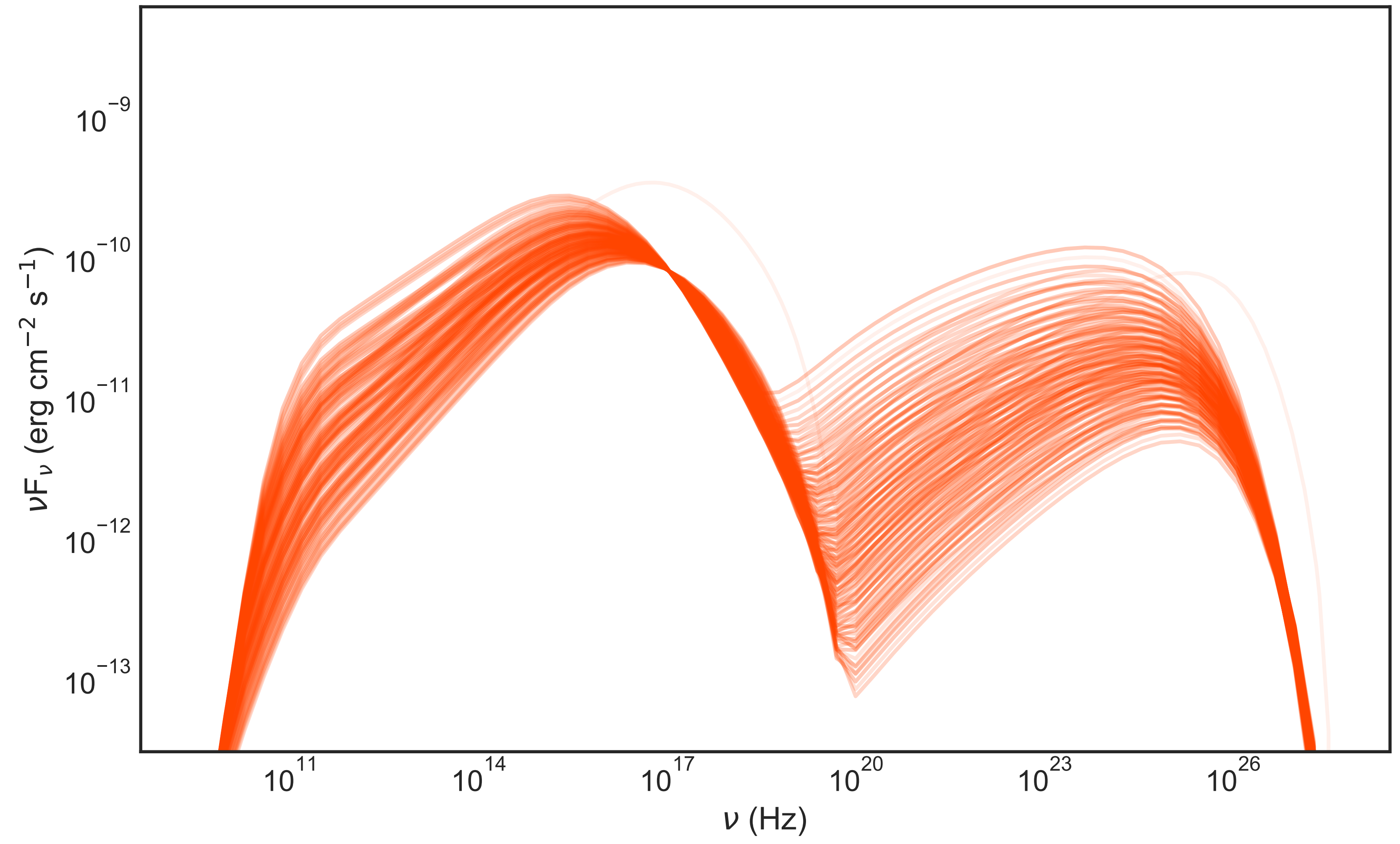

External inverse Compton

10^6 parameter sets → SOPRANO →

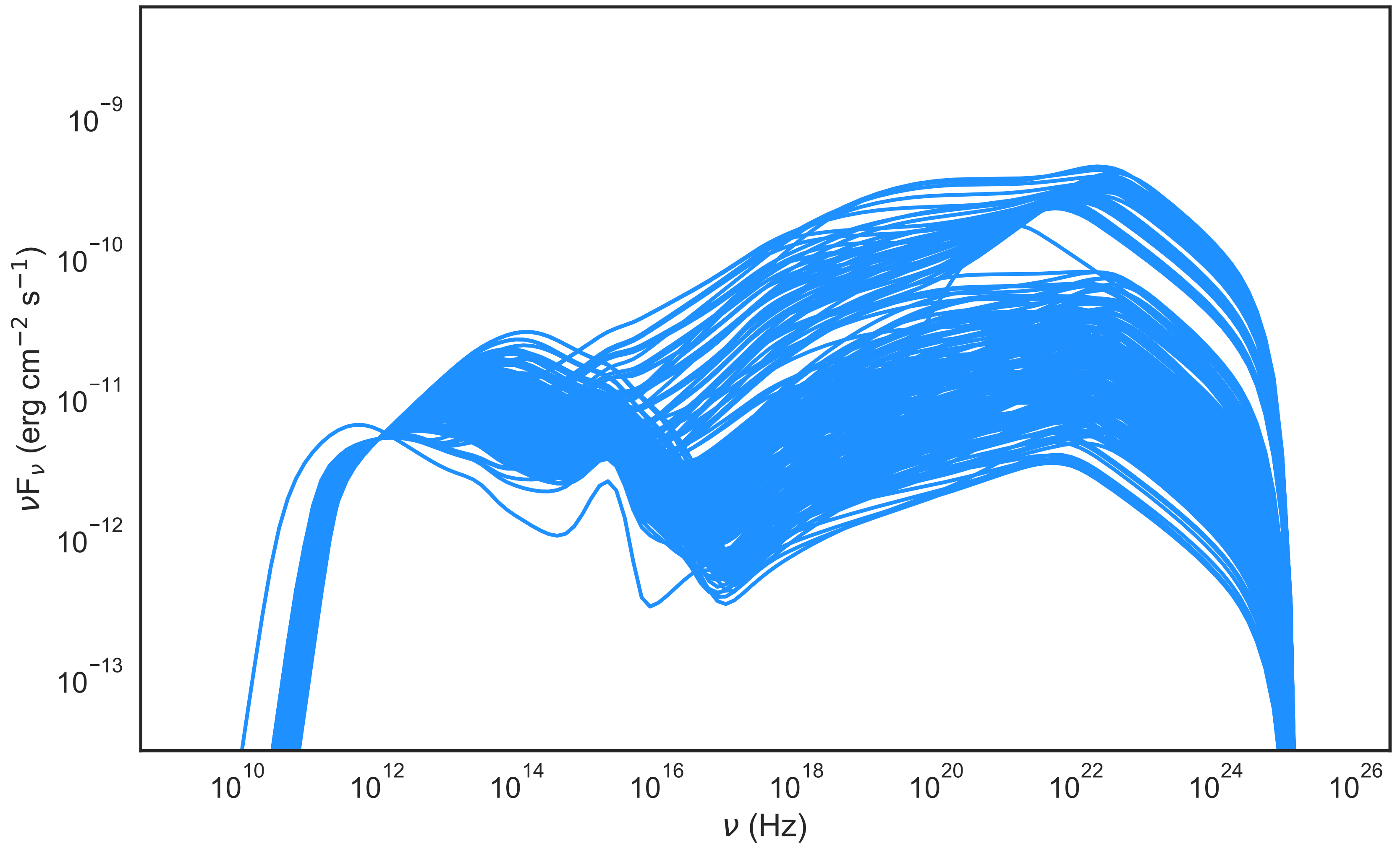

Scalable

- From 1 job to 20 million jobs in queue

Small, Quick

- Small memory footprint
- Speed: clocked up to 70k+ tasks/second

Feature Rich

- Full-cycle scheduler
- Cost-driven job placement
- Workload analysis (via simulation)
- Prediction of job duration + job size
- PMIx support (evolution of MPI)
- SAGA (storage-aware scheduling)
- Rapid Scaling in cloud

FNC is the synthesis of decades of experience with jobs schedulers

PBS + Grid Engine + Accelerator

ALTAIR

Contact: casotto@altair.com

REPORT BY user FOR SET

Soprano:ALL

	Jobs	Unknown Duration	Count (%)	Total Time	Time (%)	Average Duration	Longest Job
total	1,000,000	0	100.00%	1y66d	100.00%	37s	27m29s
ncadmin	1,000,000	0	100.00%	1y66d	100.00%	37s	27m29s

First Job Start	Wed Oct 25 09:15:59 2023
Last Job Finish	Thu Oct 26 02:41:36 2023
Elapsed Time	17h25m

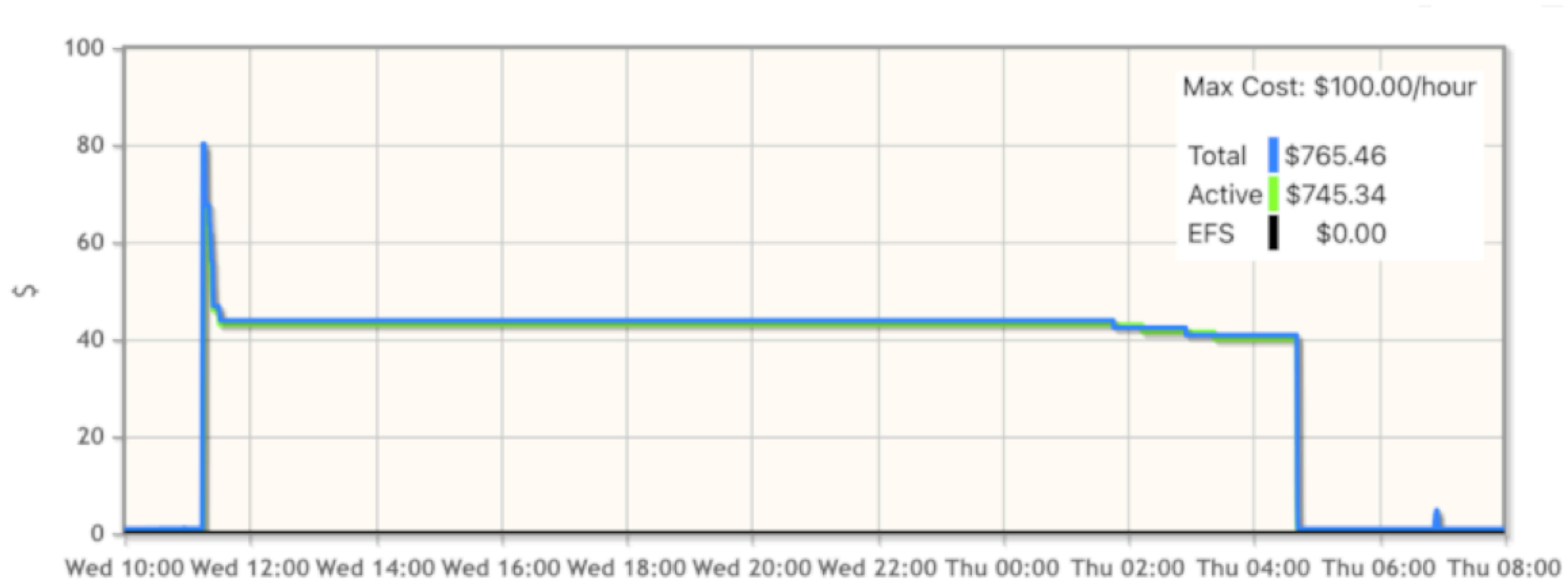

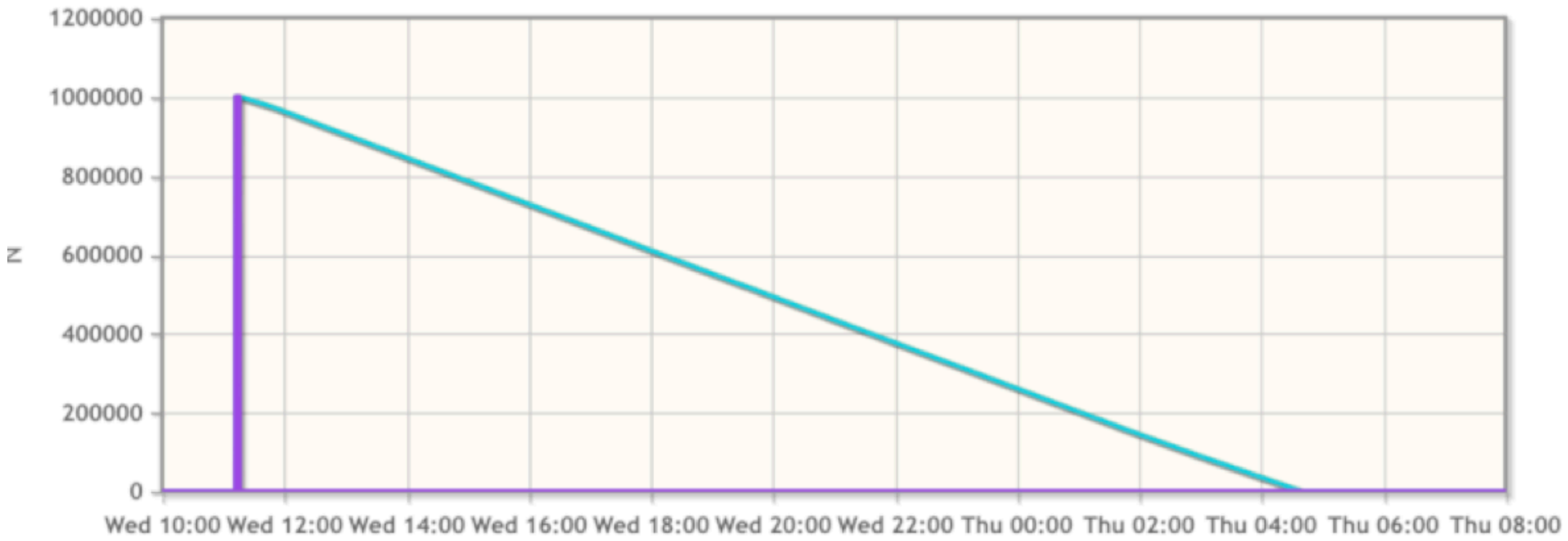

		Status	Size	Duration	Actions
	[..]				
	[ALL]				
1	ALL	999955 45	1,000,000	1y66d	
2	Batch0000	25000	25,000	13d03h	
3	Batch0001	25000	25,000	10d17h	
4	Batch0002	25000	25,000	10d15h	
5	Batch0003	25000	25,000	10d16h	
6	Batch0004	25000	25,000	10d15h	
7	Batch0005	25000	25,000	10d16h	
8	Batch0006	25000	25,000	10d15h	
9	Batch0007	25000	25,000	10d15h	
10	Batch0008	25000	25,000	10d16h	
11	Batch0009	25000	25,000	10d16h	
12	Batch0010	25000	25,000	10d17h	
13	Batch0011	25000	25,000	10d15h	
14	Batch0012	25000	25,000	10d15h	
15	Batch0013	25000	25,000	10d14h	
16	Batch0014	25000	25,000	10d16h	
17	Batch0015	25000	25,000	10d15h	
18	Batch0016	25000	25,000	10d15h	
19	Batch0017	25000	25,000	10d15h	
20	Batch0018	25000	25,000	10d14h	
21	Batch0019	25000	25,000	10d20h	
22	Batch0020	25000	25,000	10d14h	
23	Batch0021	25000	25,000	10d15h	
24	Batch0022	25000	25,000	10d15h	
25	Batch0023	25000	25,000	10d18h	
26	Batch0024	25000	25,000	10d17h	
27	Batch0025	25000	25,000	10d18h	
28	Batch0026	25000	25,000	10d18h	
29	Batch0027	25000	25,000	10d18h	
30	Batch0028	25000	25,000	10d17h	
31	Batch0029	25000	25,000	10d17h	
32	Batch0030	25000	25,000	10d16h	
33	Batch0031	25000	25,000	10d17h	
34	Batch0032	25000	25,000	10d18h	
35	Batch0033	24978 22	25,000	11d03h	
36	Batch0034	25000	25,000	10d18h	
37	Batch0035	25000	25,000	10d20h	
38	Batch0036	24977 23	25,000	11d04h	
39	Batch0037	25000	25,000	10d18h	
40	Batch0038	25000	25,000	10d20h	
41	Batch0039	25000	25,000	10d19h	

Monitoring the data

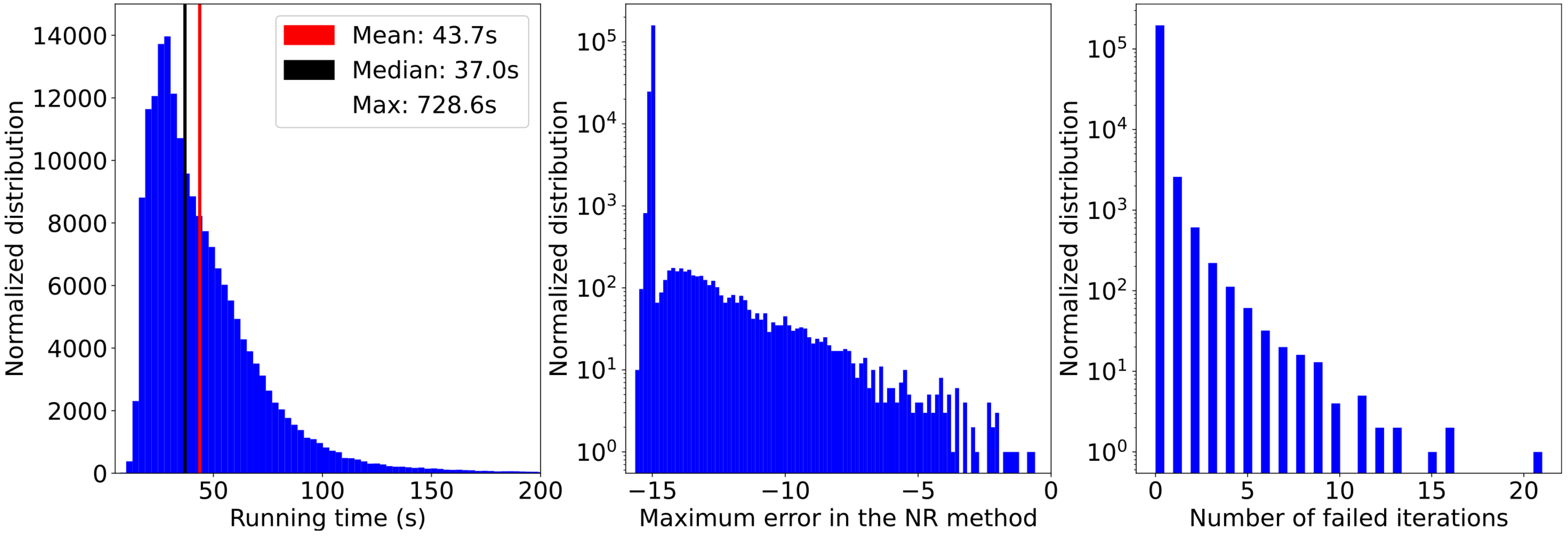

The average simulation time is 43.7 s per spectra, with a long tail extending beyond 700 s. These extended durations correspond to spectra characterized by a high compactness with small radius R, large electron luminosity Le, and small injection Lorentz factor gmin.

Bégué, Sahakyan, et al., 2024, ApJ, 963, id.71

The computation of the spectra by SOPRANO can fail. The solution is obtained with the Newton–Raphson root finding algorithm, which can, in some instances, not converge toward the solution with the required accuracy (10^{-15}), close to machine accuracy. The total number of spectra with at least one failed time iteration is 3693, constituting fewer than 2% of all calculated spectra. From the distribution of the maximum error across a full simulation is evident that only a small fraction of the spectra are unreliable, with most spectra having a maximal error below 10^{-10}.

Data

Spectra from SOPRANO:
150 energy bins

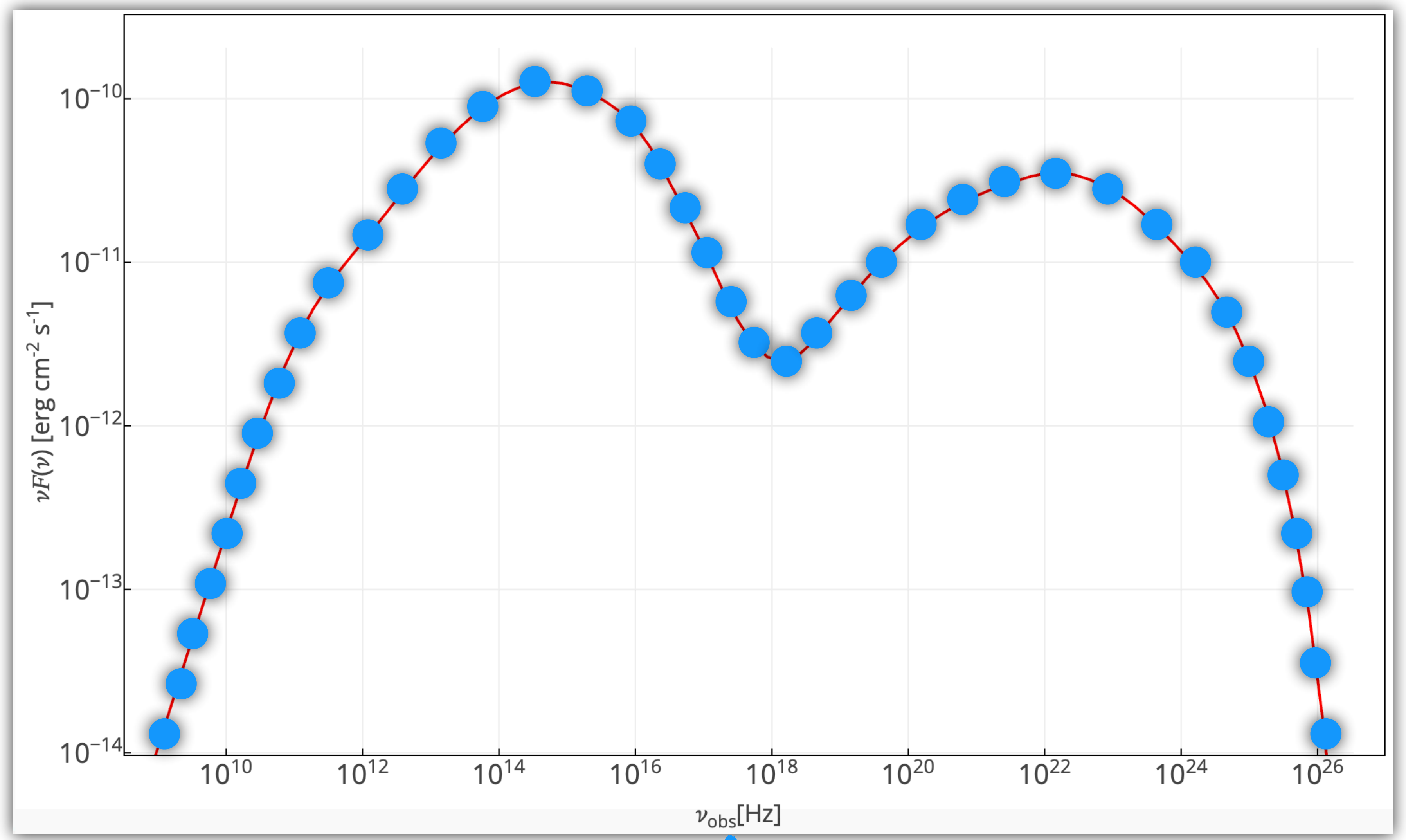

Principal component analysis

Data preparation

Step 1: log the data
Step 2: remove the mean
Step 3: detrend
Step 4: normalise amplitude to [-1,1]

train

$P_1 \ldots\ldots P_7$

Modeling the relationship between the input parameters and their corresponding spectra

Convolutional Neural Networks (CNNs)

CNNs, initially designed for image analysis, have evolved to become versatile tools for processing sequential data, including time series. Their ability to automatically extract hierarchical features makes them well-suited for capturing complex temporal dependencies present in time series data.

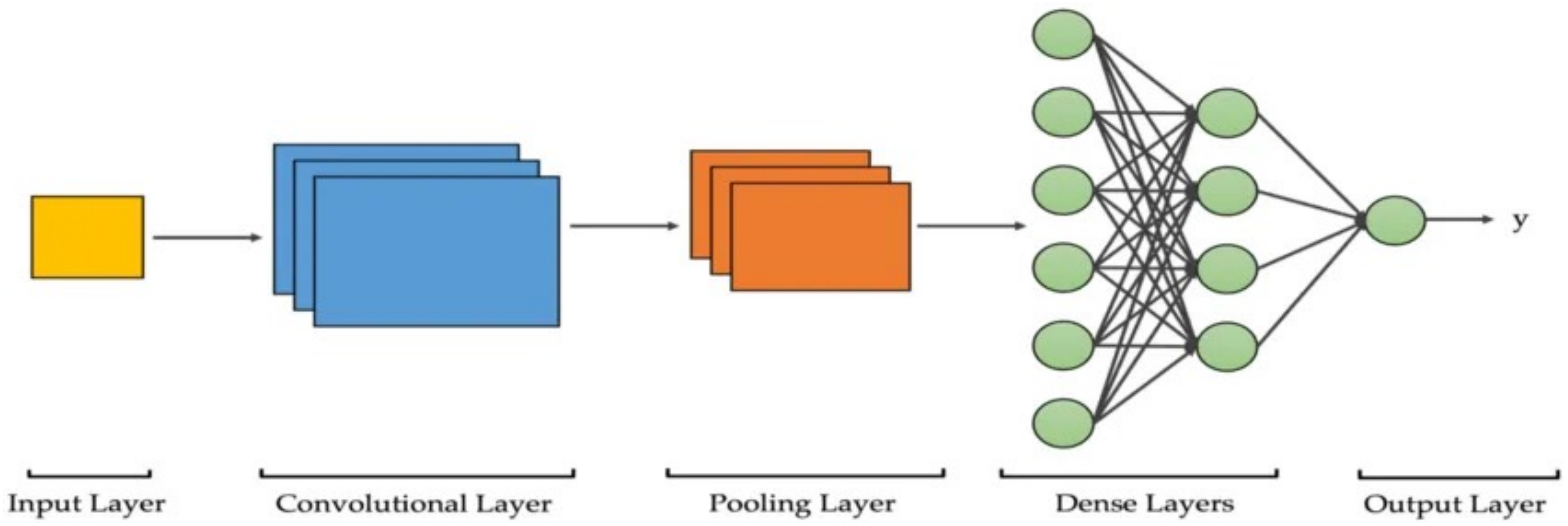

The neural network

Input

Independent outputs

The neural network

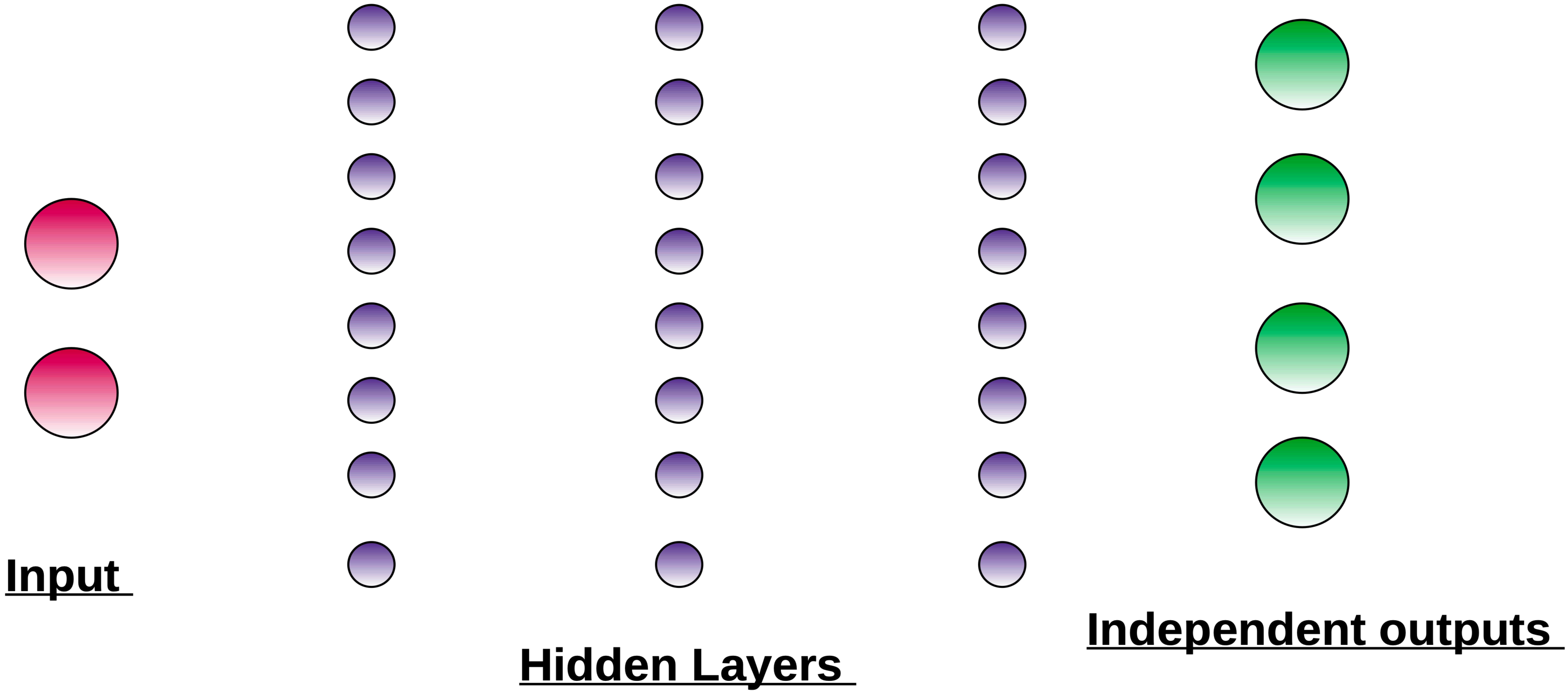

The neural network

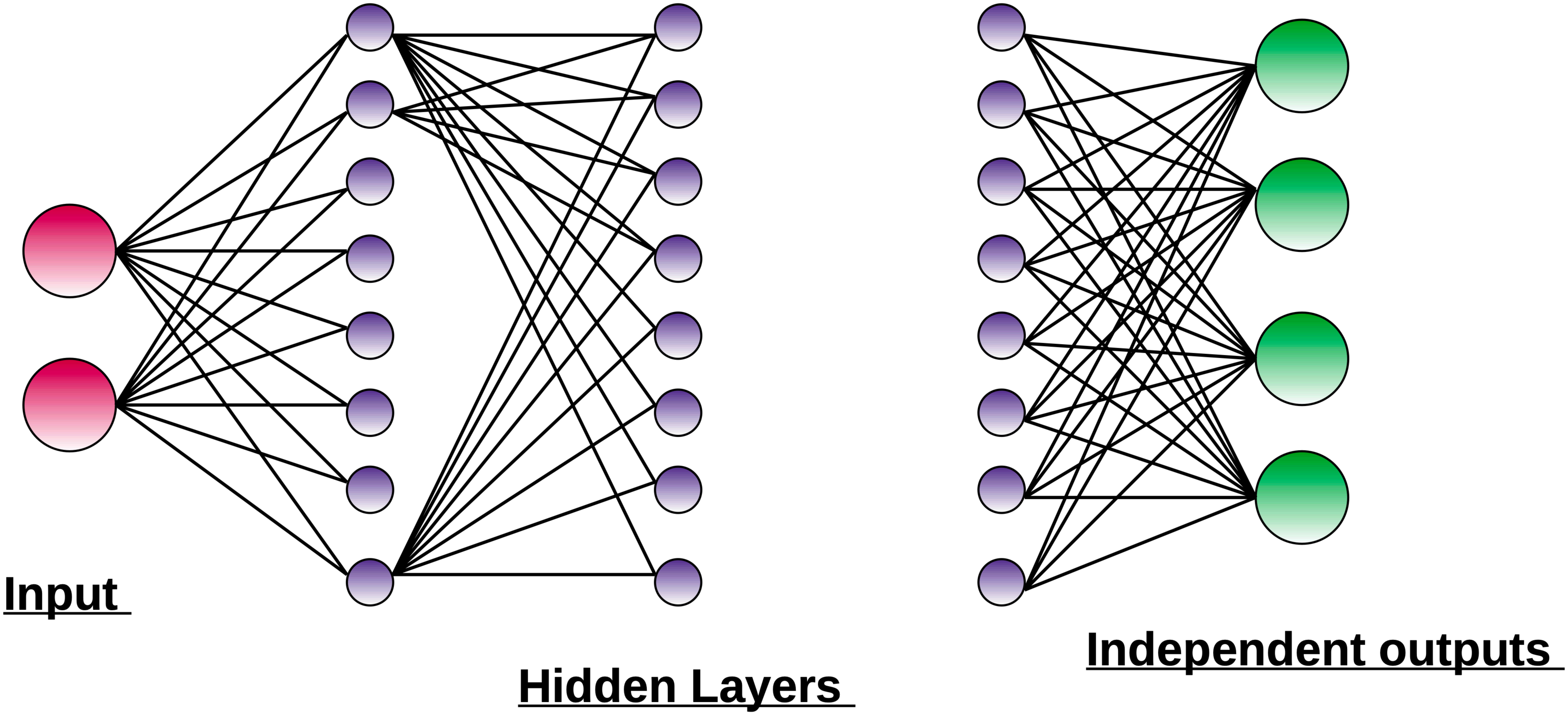

The neural network

A deep network is not necessary to produce an accurate representation of the numerical model. The CNN contains only eight layers in this order: a first dense layer transforms the seven inputs to a high dimensional vector, five 1D convolutional layers with different kernel sizes and strides, one maxpooling layer followed by a 1D convolutional layer, and a final dense layer, mapping to the 150 outputs.

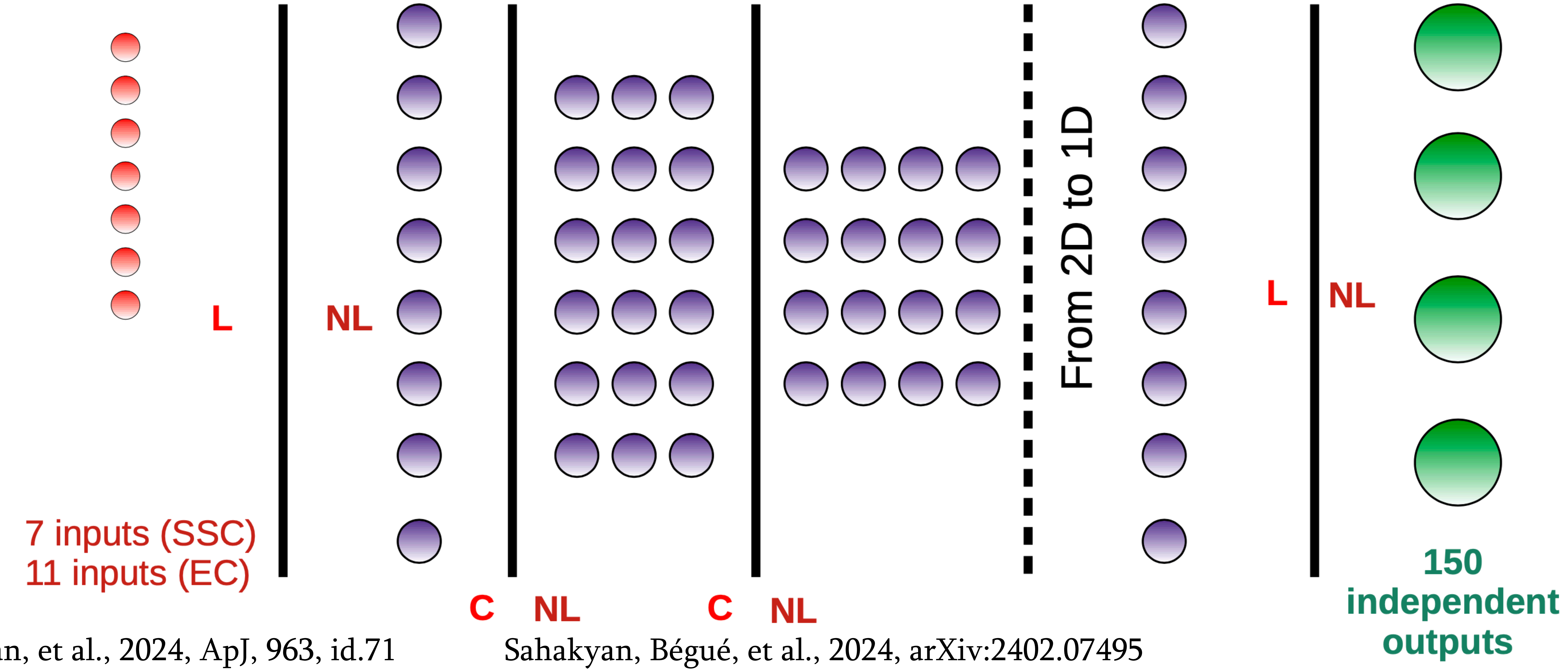

Bégué, Sahakyan, et al., 2024, ApJ, 963, id.71

Sahakyan, Bégué, et al., 2024, arXiv:2402.07495

Final results

Our sample of spectra is split into a 80% training set, a 10% validation set, and a 10% test set.

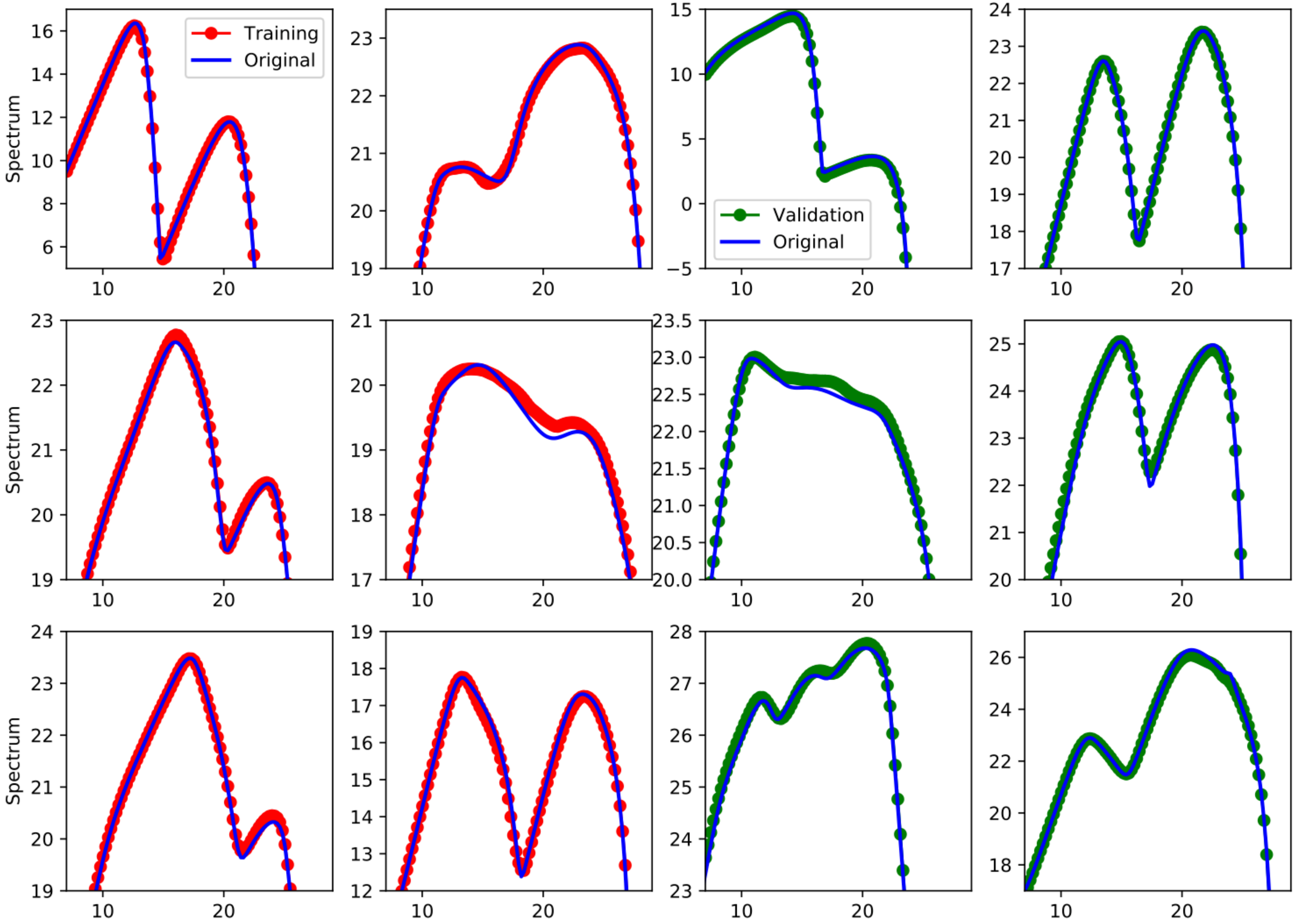

Bégué, Sahakyan, et al., 2024, ApJ, 963, id.71

Workflow of the method

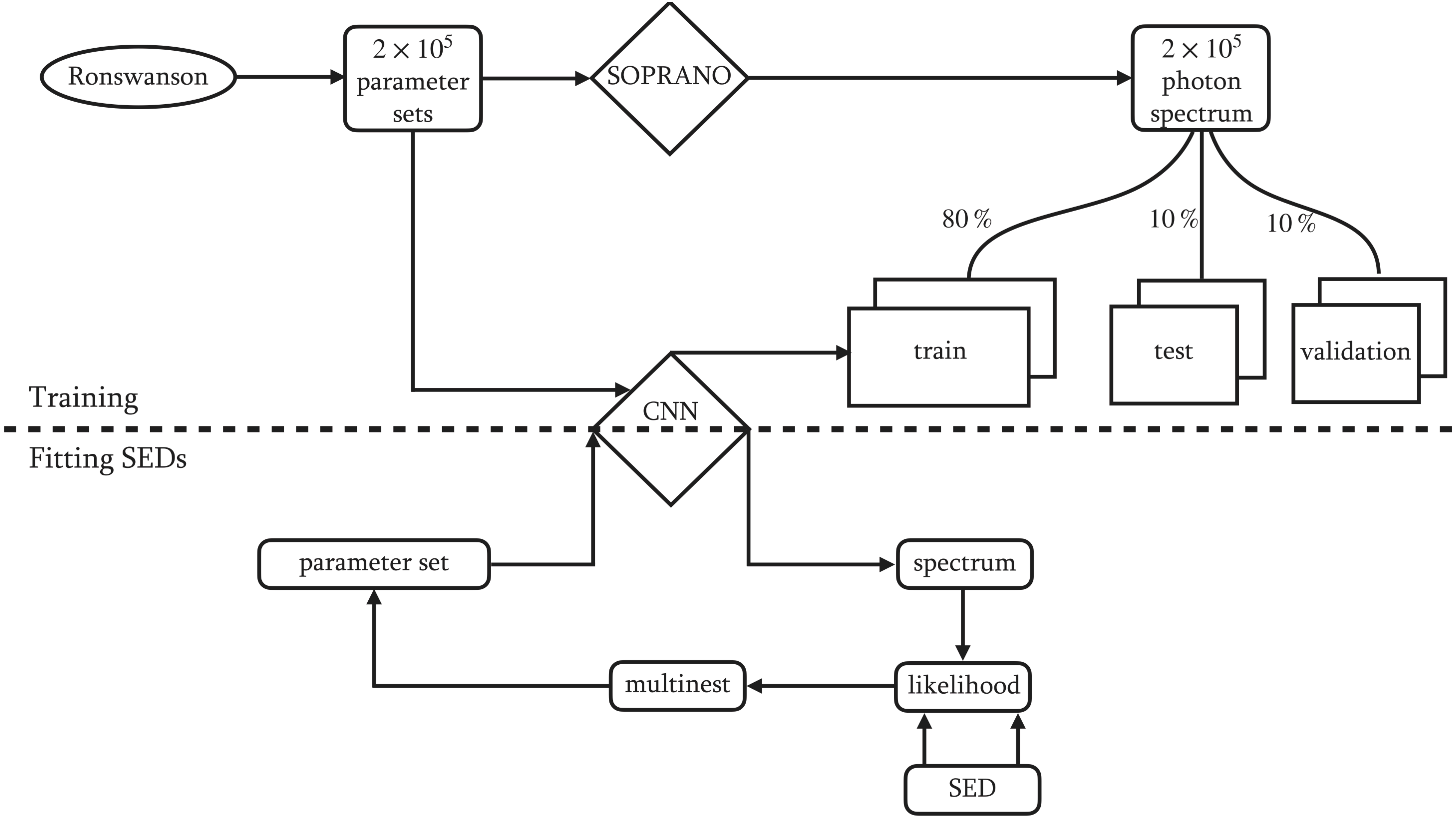

Bégué, Sahakyan, et al., 2024, ApJ, 963, id.71

Workflow of the method

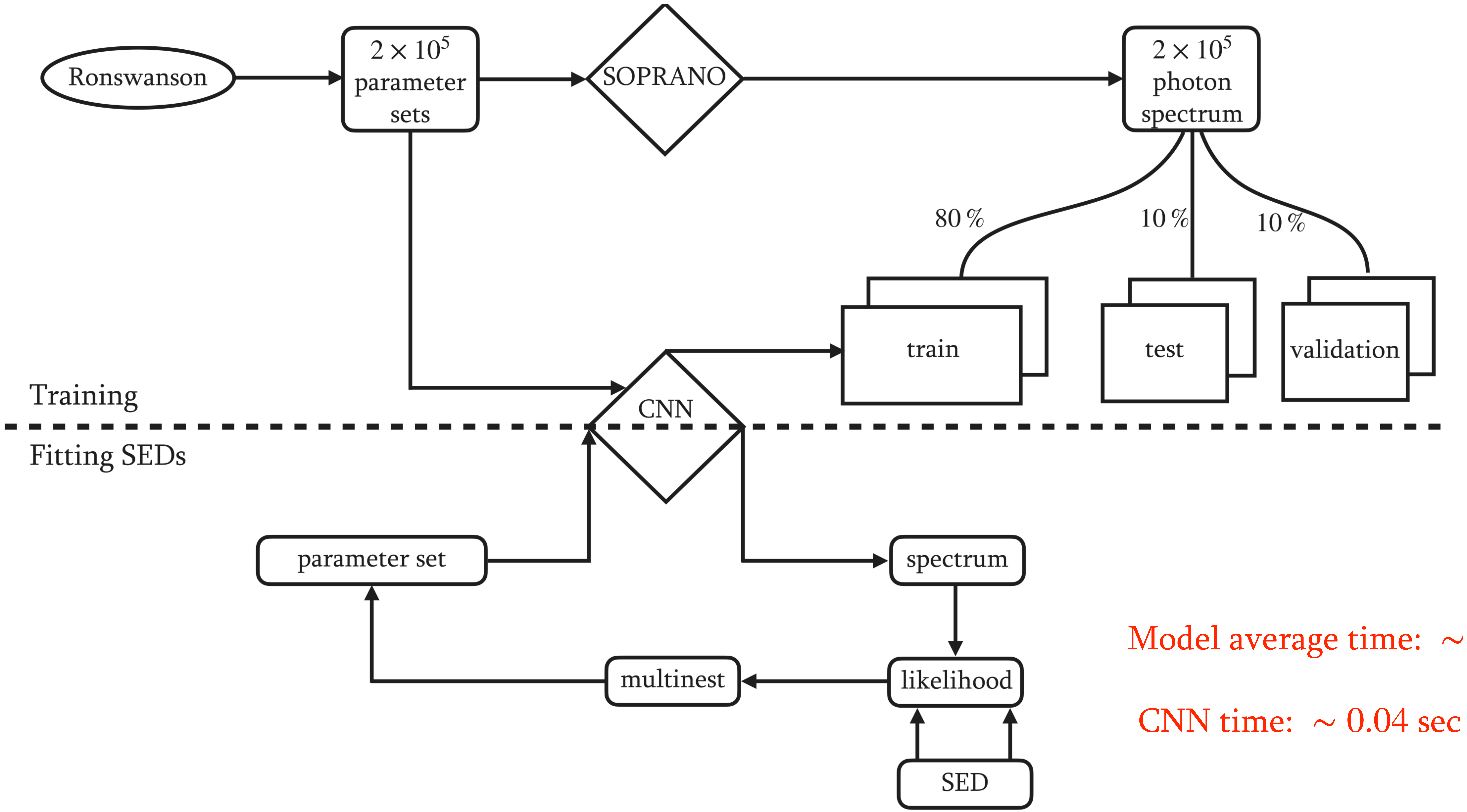

Model average time: $\sim$ 30 sec

CNN time: $\sim$ 0.04 sec

Bégué, Sahakyan, et al., 2024, ApJ, 963, id.71

Application

The trained CNN is used with multinest to fit the broadband SEDs of 4 blazars

BL Lacs

The emission lines are weak or absent

- ☑ Mrk 421
- ☑ 1ES 1959+650

FSRQs

Strong emission lines

- ☑ 3C 454.3
- ☑ CTA 102

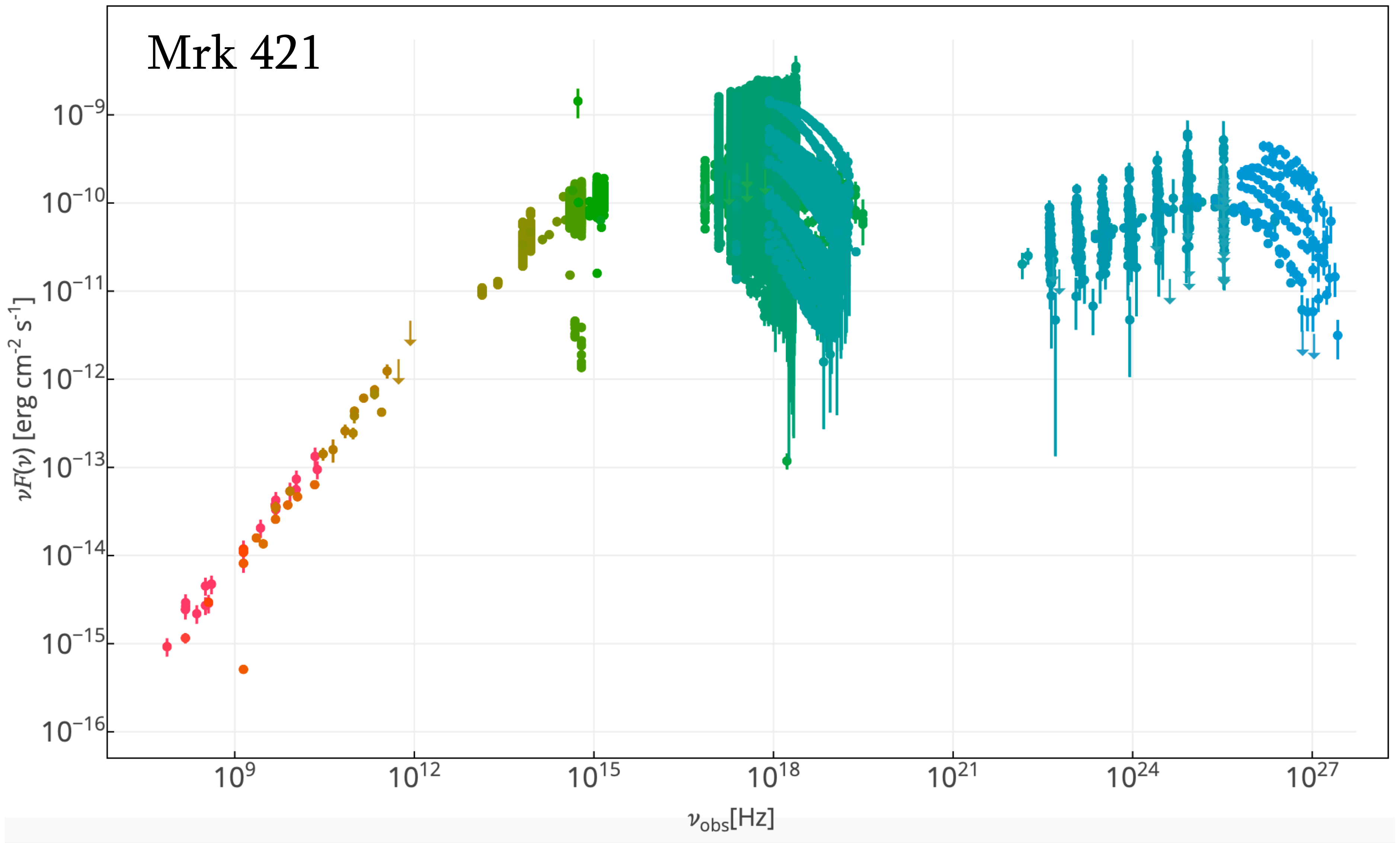

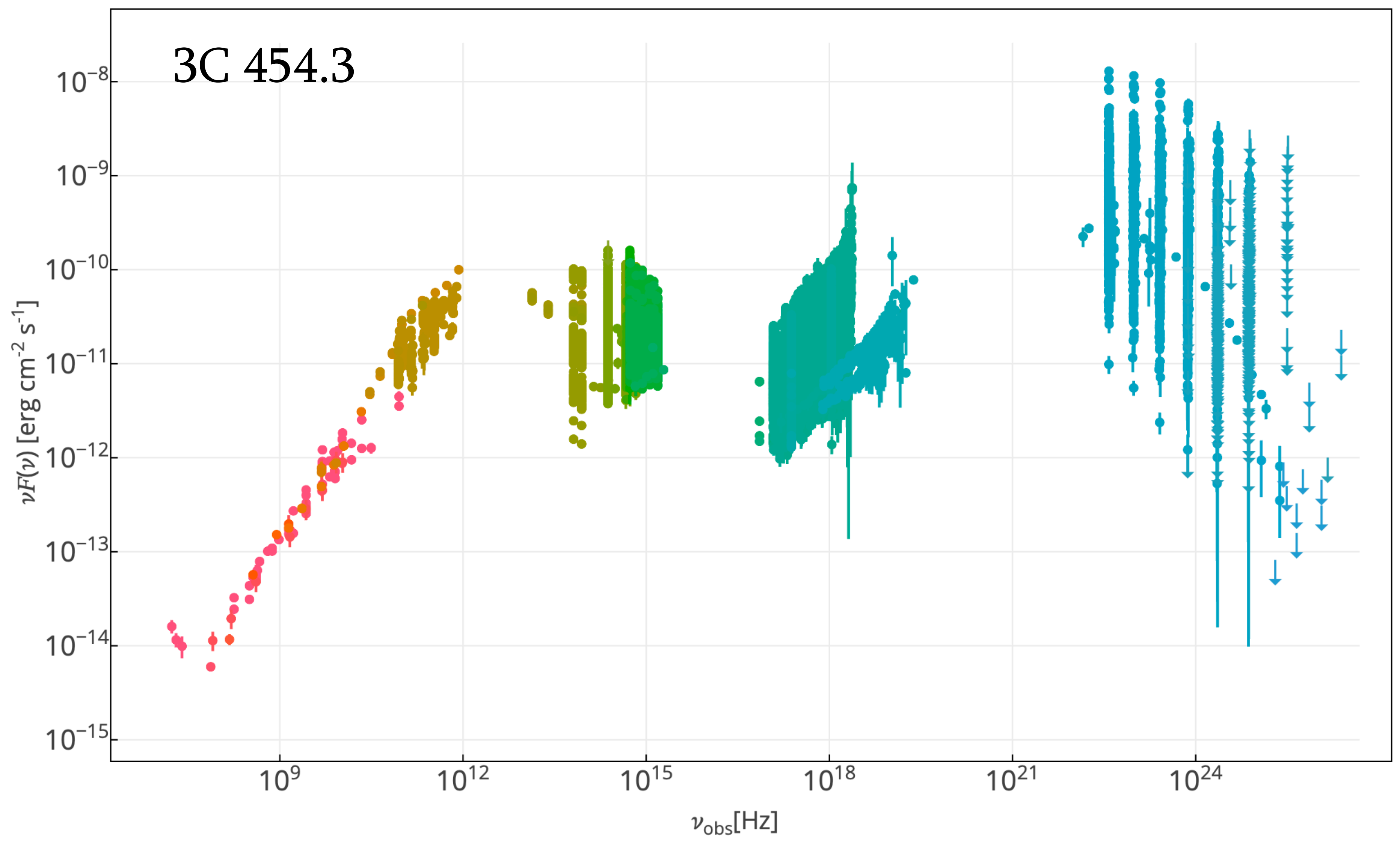

Results

Synchrotron self-Compton model

- Mrk 421 (**z = 0.031, data from MW campaign in 2009**)

  1ES 1959+650

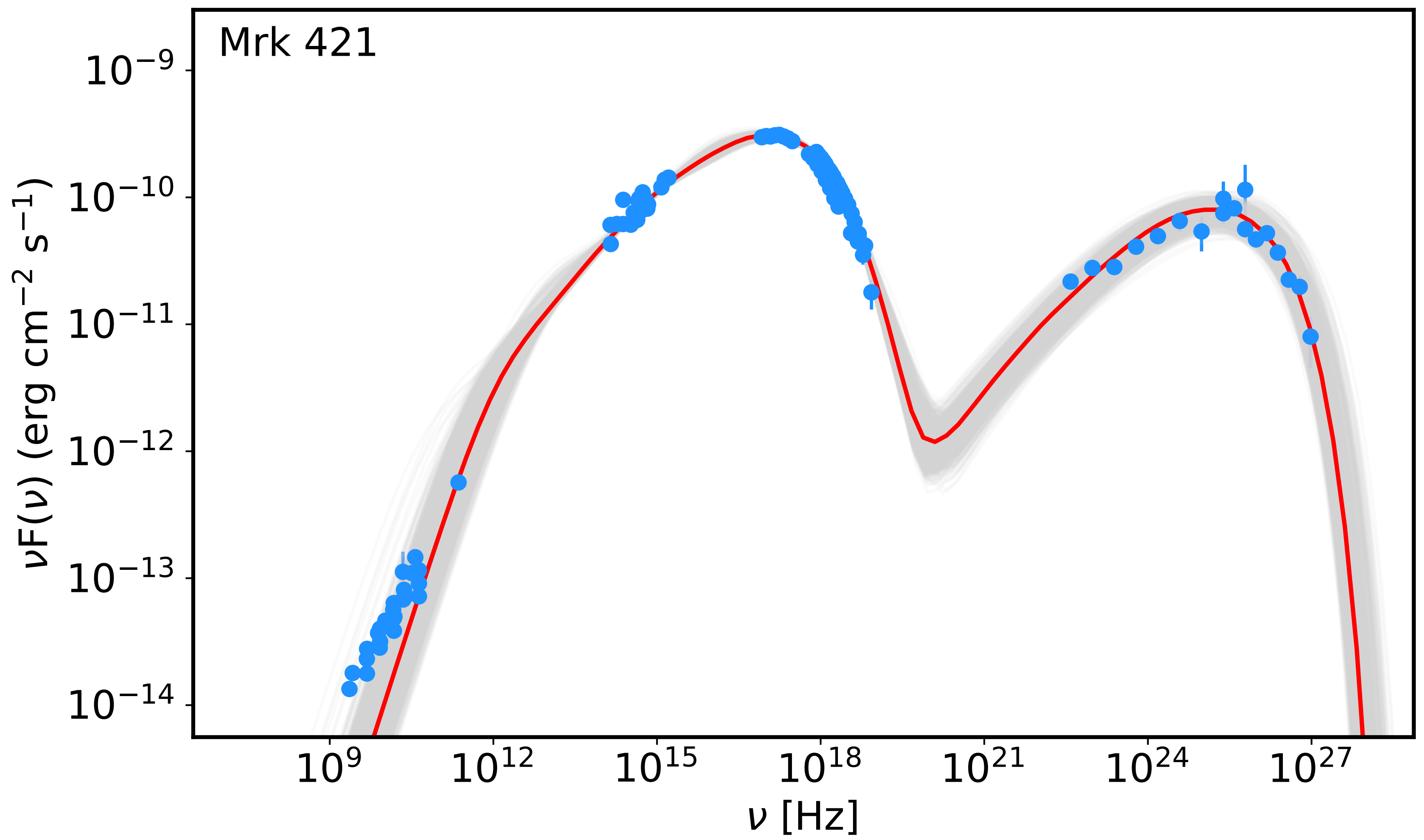

The broadband SEDs of Mrk 421 during the 4.5 month long multiwavelength campaign in 2009. The data and the errors are in blue, the red line is the model corresponding to the best parameters, i.e., maximizing the likelihood, and the gray spectra represent one in 10 randomly selected samples from the MCMC sampling, representing the model uncertainty.

Bégué, Sahakyan, et al., 2024, ApJ, 963, id.71

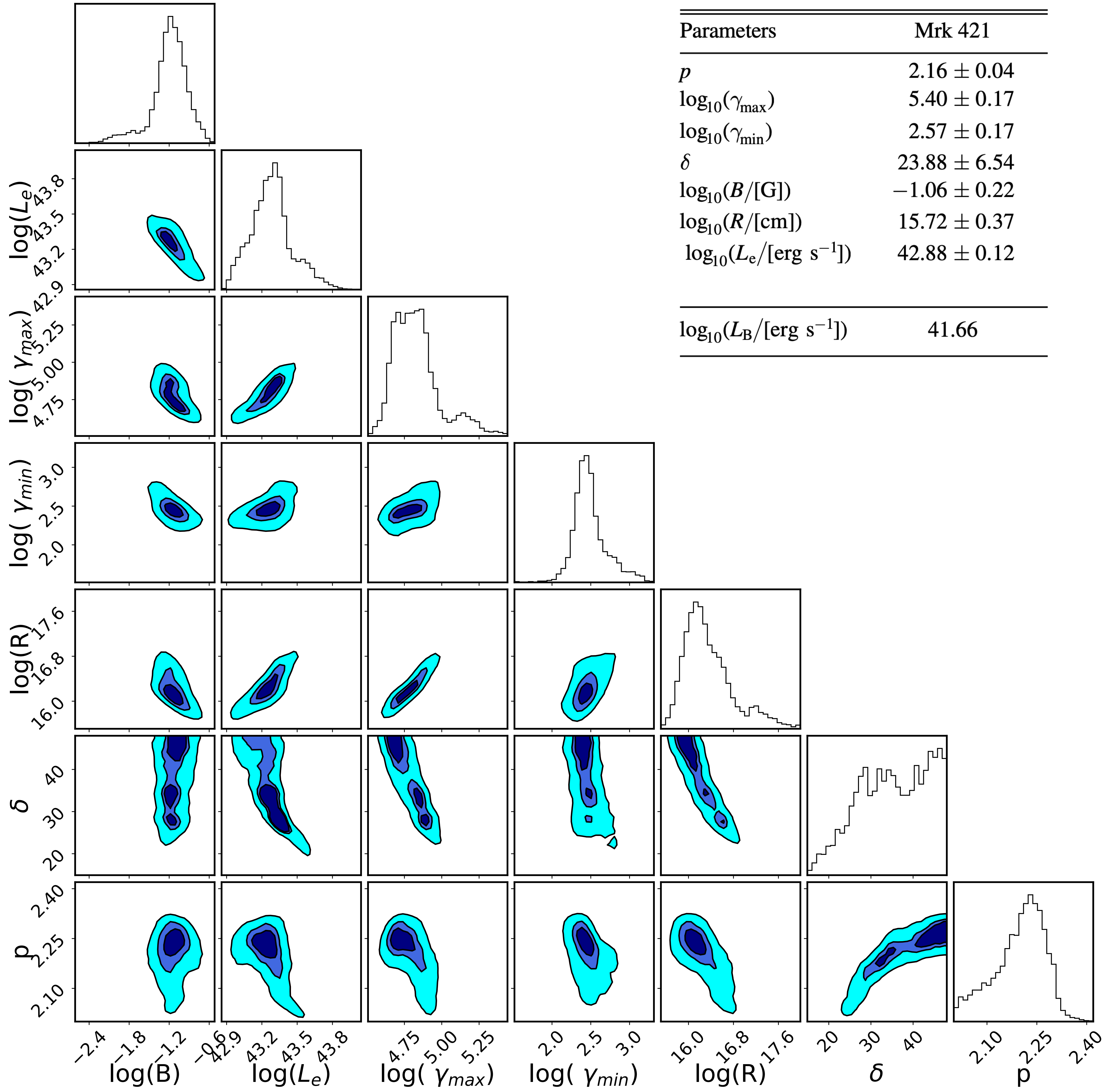

Parameters	Mrk 421
p	2.16 ± 0.04
$\log_{10}(\gamma_{\rm max})$	5.40 ± 0.17
$\log_{10}(\gamma_{\rm min})$	2.57 ± 0.17
δ	23.88 ± 6.54
$\log_{10}(B/[\rm G])$	-1.06 ± 0.22
$\log_{10}(R/[\rm cm])$	15.72 ± 0.37
$\log_{10}(L_e/[\rm erg\ s^{-1}])$	42.88 ± 0.12
$\log_{10}(L_B/[\rm erg\ s^{-1}])$	41.66

Parameter posterior distributions for Mrk 421 during the multiwavelength campaign of 2009. The contours give, from outward to inward, the 20%, 40%, and 75% confidence regions. Apart from the radius R, all parameters are well constrained.

Results

Synchrotron self-Compton model

Mrk 421

- 1ES 1959+650 (**z = 0.031, data from MW campaign in 2009**)

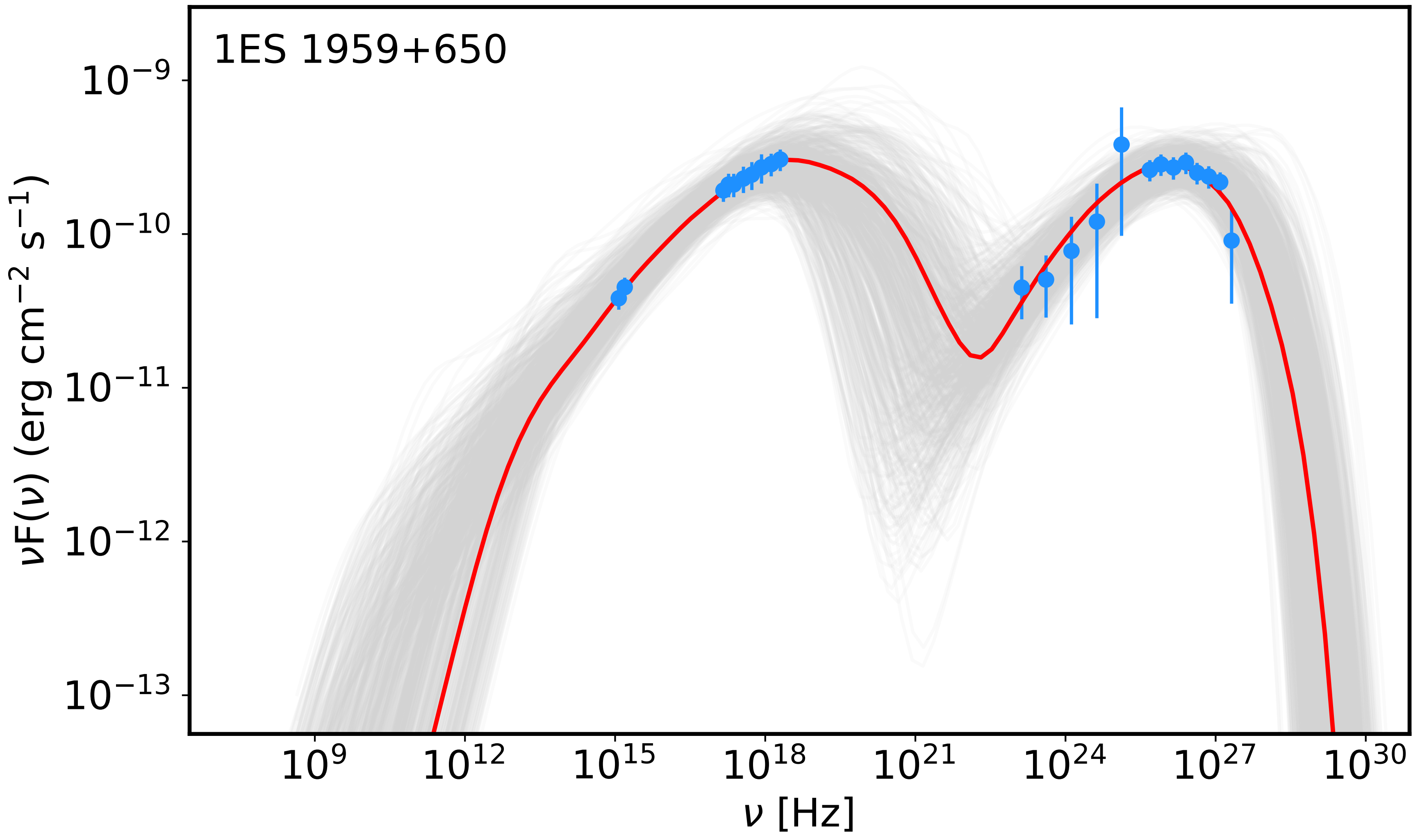

The broadband SEDs of 1ES 1959+650 on the 2016 June 14 . The data and the errors are in blue, the red line is the model corresponding to the best parameters, i.e., maximizing the likelihood, and the gray spectra represent one in 10 randomly selected samples from the MCMC sampling, representing the model uncertainty.

Bégué, Sahakyan, et al., 2024, ApJ, 963, id.71

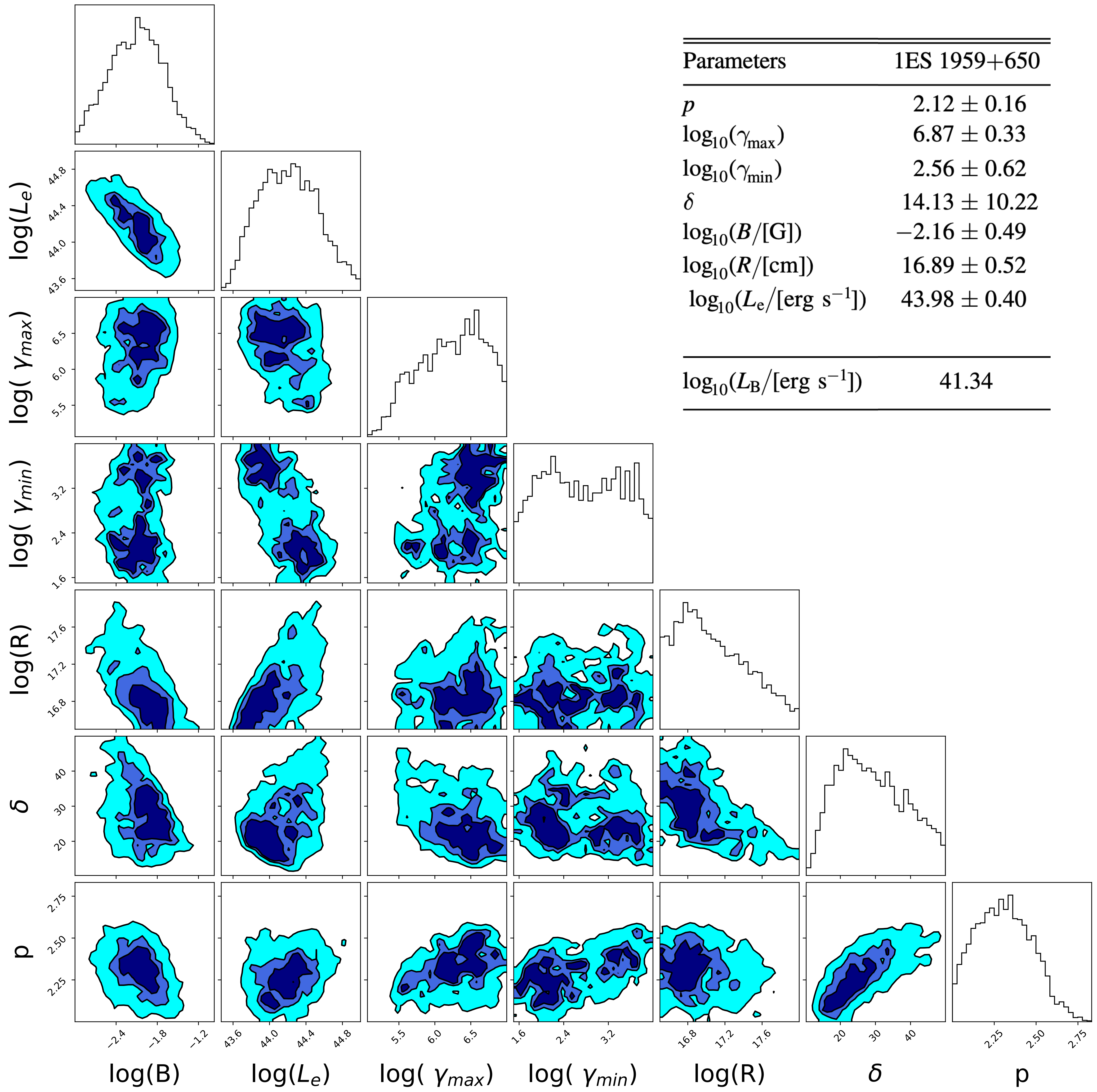

Parameters	1ES 1959+650
p	2.12 ± 0.16
$\log_{10}(\gamma_{\rm max})$	6.87 ± 0.33
$\log_{10}(\gamma_{\rm min})$	2.56 ± 0.62
δ	14.13 ± 10.22
$\log_{10}(B/[{\rm G}])$	-2.16 ± 0.49
$\log_{10}(R/[{\rm cm}])$	16.89 ± 0.52
$\log_{10}(L_e/[{\rm erg\ s^{-1}}])$	43.98 ± 0.40
$\log_{10}(L_B/[{\rm erg\ s^{-1}}])$	41.34

Parameter posterior distributions for 1ES 1959+650. The magnetic field, the electron luminosity, and the electron index are well constrained. In contrast, the other parameters remain somewhat unconstrained due to the high uncertainty in the position of the peak energy of the synchrotron bump.

Results

External inverse Compton

- 3C 454.3 (**z = 0.859**)

  CTA 102

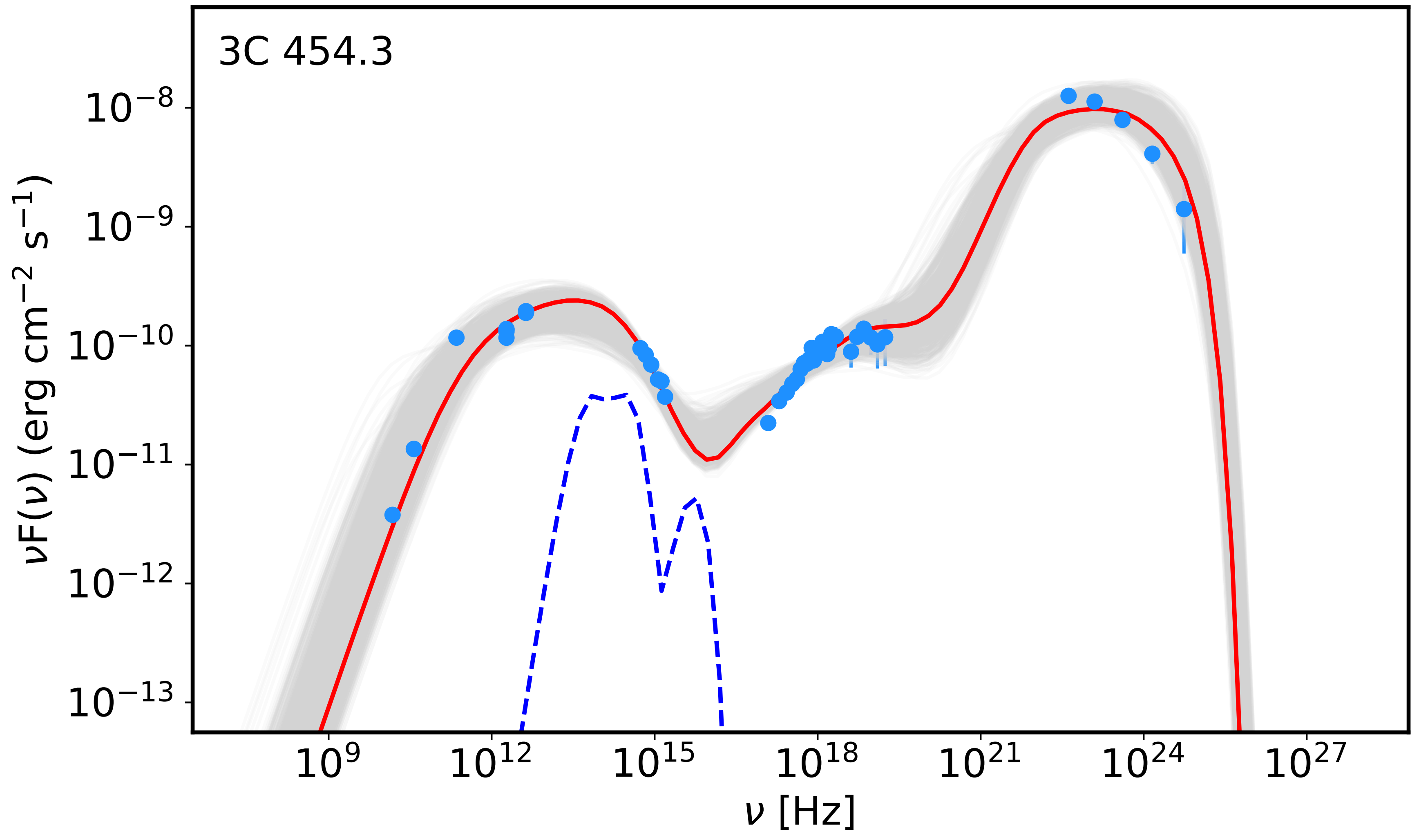

Multiwavelength SED of 3C 454.3, presented in blue. The model corresponding to the maximum likelihood is shown by the solid red line, while the uncertainty associated with the model is depicted in gray.

Sahakyan, Bégué, et al., 2024, arXiv:2402.07495

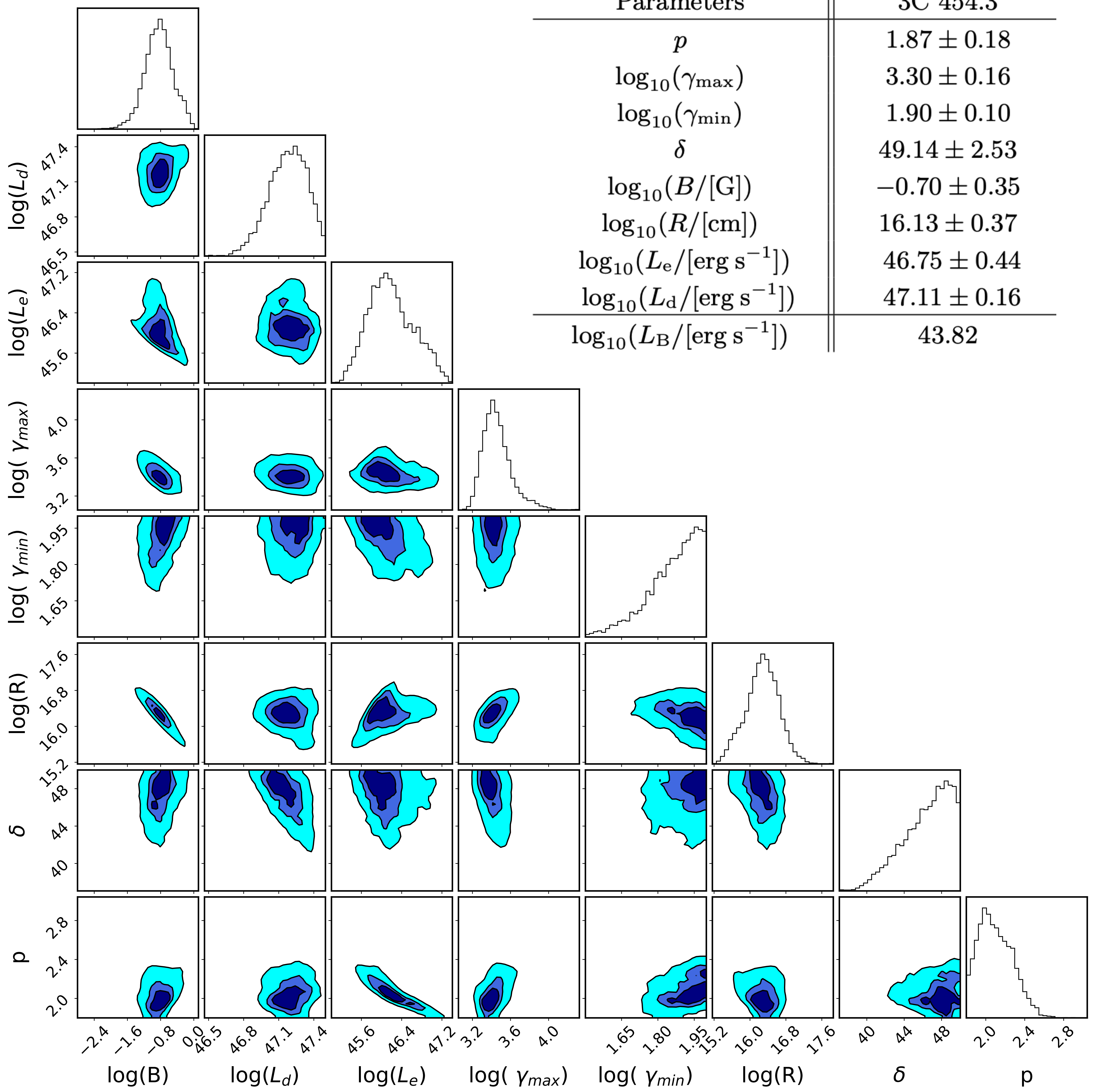

Parameters	3C 454.3
p	1.87 ± 0.18
$\log_{10}(\gamma_{\max})$	3.30 ± 0.16
$\log_{10}(\gamma_{\min})$	1.90 ± 0.10
δ	49.14 ± 2.53
$\log_{10}(B/[\mathrm{G}])$	-0.70 ± 0.35
$\log_{10}(R/[\mathrm{cm}])$	16.13 ± 0.37
$\log_{10}(L_e/[\mathrm{erg\ s^{-1}}])$	46.75 ± 0.44
$\log_{10}(L_\mathrm{d}/[\mathrm{erg\ s^{-1}}])$	47.11 ± 0.16
$\log_{10}(L_\mathrm{B}/[\mathrm{erg\ s^{-1}}])$	43.82

Parameter posterior distributions from the SED modeling of 3C 454.3 for the period MJD 55519.59-55520.19

Results

External inverse Compton

3C 454.3

➡ CTA 102 (**z = 1.037**)

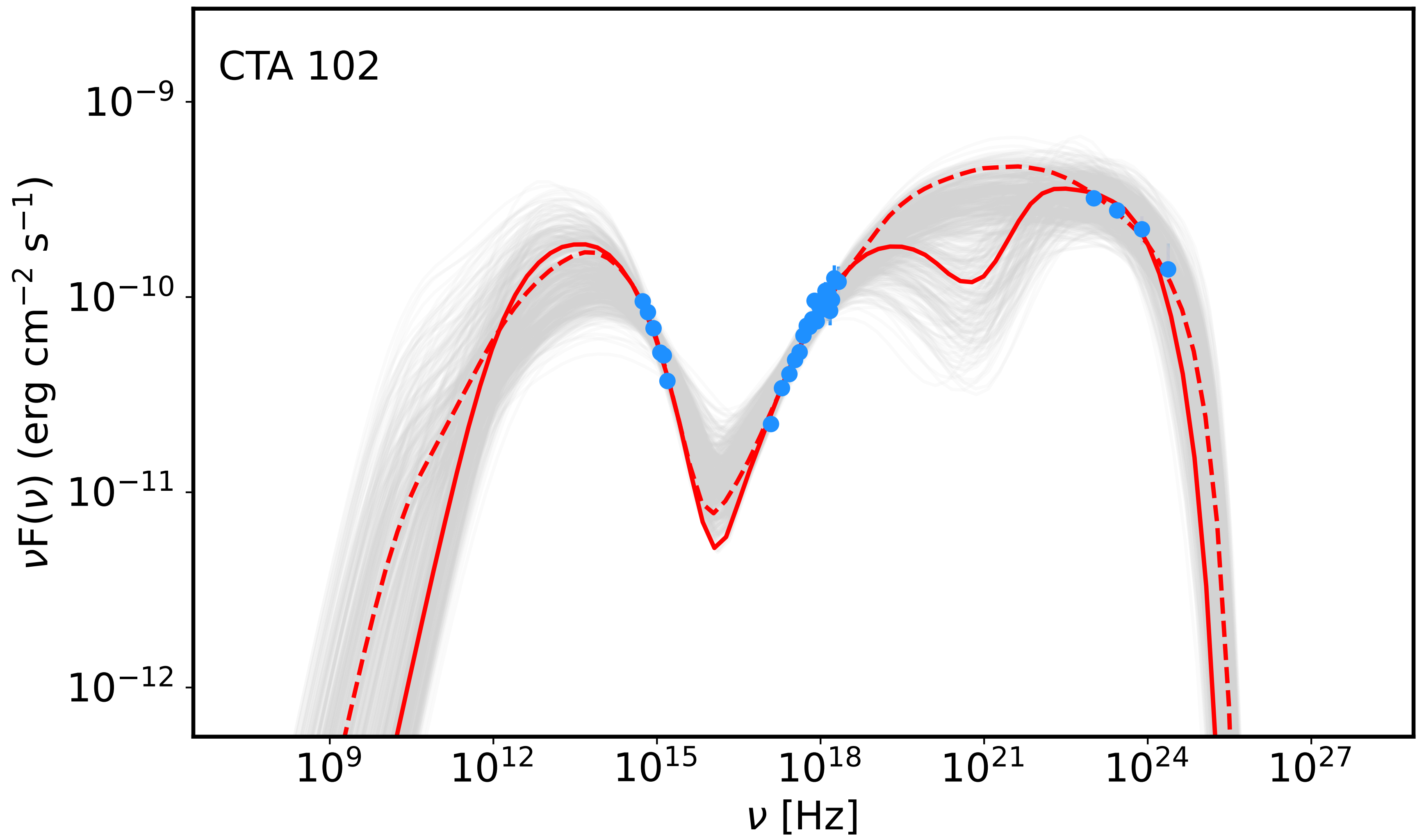

Multiwavelength SED of CTA 102, presented in blue. The model corresponding to the maximum likelihood is shown by the solid red line, while the uncertainty associated with the model is depicted in gray. the red dashed line represents the scenario for which the radius is larger and the emission is due to SSC

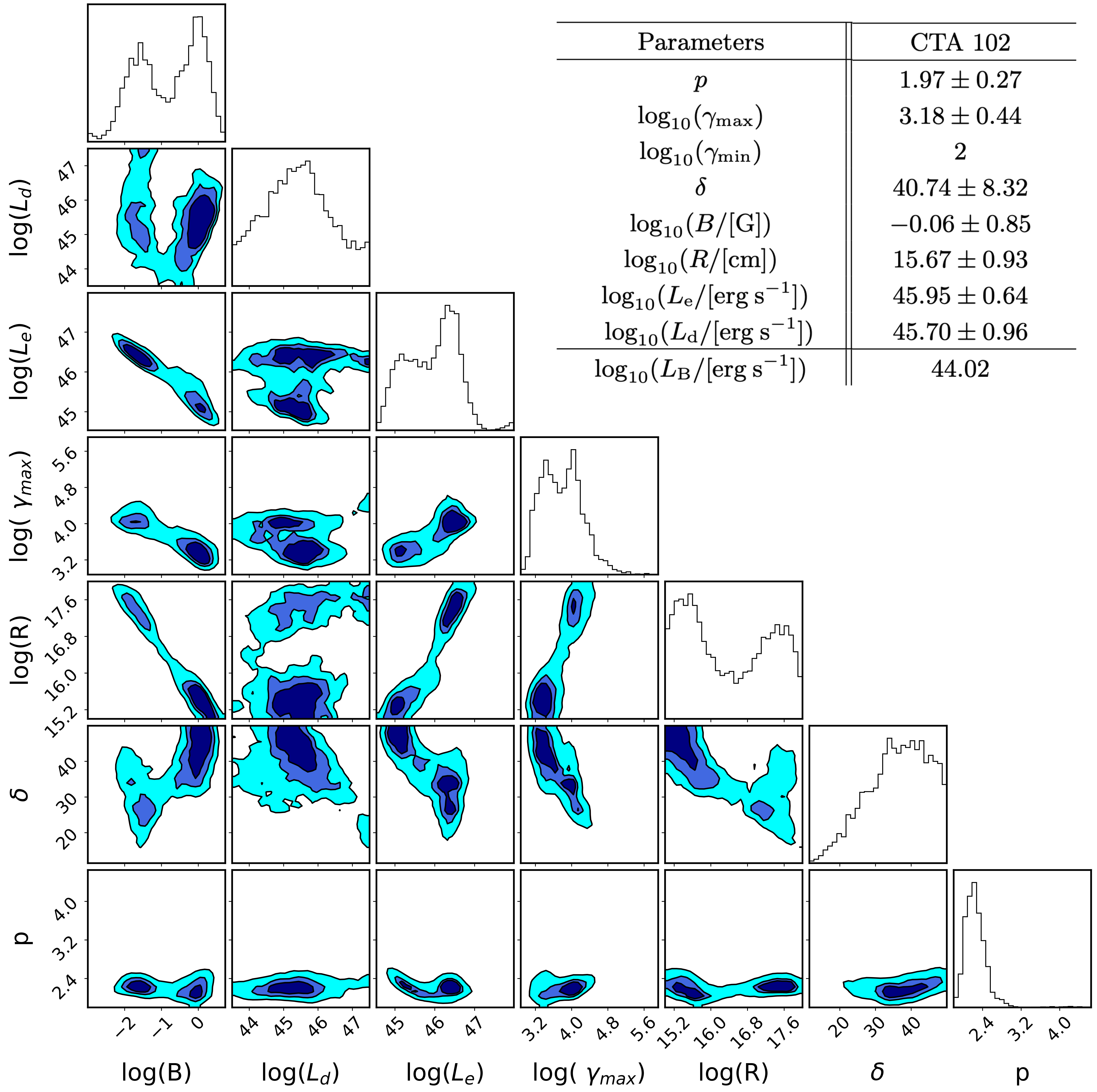

Parameters	CTA 102
p	1.97 ± 0.27
$\log_{10}(\gamma_{\rm max})$	3.18 ± 0.44
$\log_{10}(\gamma_{\rm min})$	2
δ	40.74 ± 8.32
$\log_{10}(B/[{\rm G}])$	-0.06 ± 0.85
$\log_{10}(R/[{\rm cm}])$	15.67 ± 0.93
$\log_{10}(L_{\rm e}/[{\rm erg\ s^{-1}}])$	45.95 ± 0.64
$\log_{10}(L_{\rm d}/[{\rm erg\ s^{-1}}])$	45.70 ± 0.96
$\log_{10}(L_{\rm B}/[{\rm erg\ s^{-1}}])$	44.02

Parameter posterior distributions for CTA 102, showing a bimodal distribution for the radius R alongside other parameters.

Sahakyan, Bégué, et al., 2024, arXiv:2402.07495


MMDC
Home
About
Data access
Theoretical Modeling
Articles
Team
Contact
https://mmdc.am/
$\nu F(\nu)$ [erg cm^{-2} s^{-1}]
ν_{obs}[Hz]
SSC
EIC
Hadronic
p
δ
log10(γmin)
log10(γmax)
log10(B/[G])
log10(R/[cm])
log10(Le/[erg s^{-1}])
z
EBL
RUN MODEL


MMDC
Home
About
Data access
Theoretical Modeling
Articles
Team
Contact
https://mmdc.am/
$\nu F(\nu)$ [erg cm^{-2} s^{-1}]
10^{-8}
10^{-9}
10^{-10}
10^{-11}
10^{-12}
10^{-13}
10^{-14}
10^{9}
10^{12}
10^{15}
10^{18}
10^{21}
10^{24}
10^{27}
10^{30}
ν_{obs}[Hz]
log10(B/[G])
log10(R/[cm])
log10(Le/[erg s^{-1}])
z
EBL
RUN MODEL
UPLOAD FILE
email
FIT
CORNER PLOT
BEST PARAMETERS
BEST MODEL

Gmail

mail

Theoretical modeling: Your fit request for SED_MW_Mrk501_EBL_DEABS_8ul8h6x.csv is ready

Inbox ×

mailtommdc@gmail.com
to me

Thu, 18 Apr, 14:44 (9 days ago)

The fit results for your recently uploaded data are now ready for review.

To access your results, please click on the link below:

View Results

Data Retention Policy

Please note that your results, along with all associated data, will be conserved on our platform for one week. After this period, all information will be permanently erased as per our data privacy and retention policy.

Best regards,

MMDC Team

Reply Forward

MMDC

Home About Data access Theoretical Modeling Articles Team Contact

https://mmdc.am/

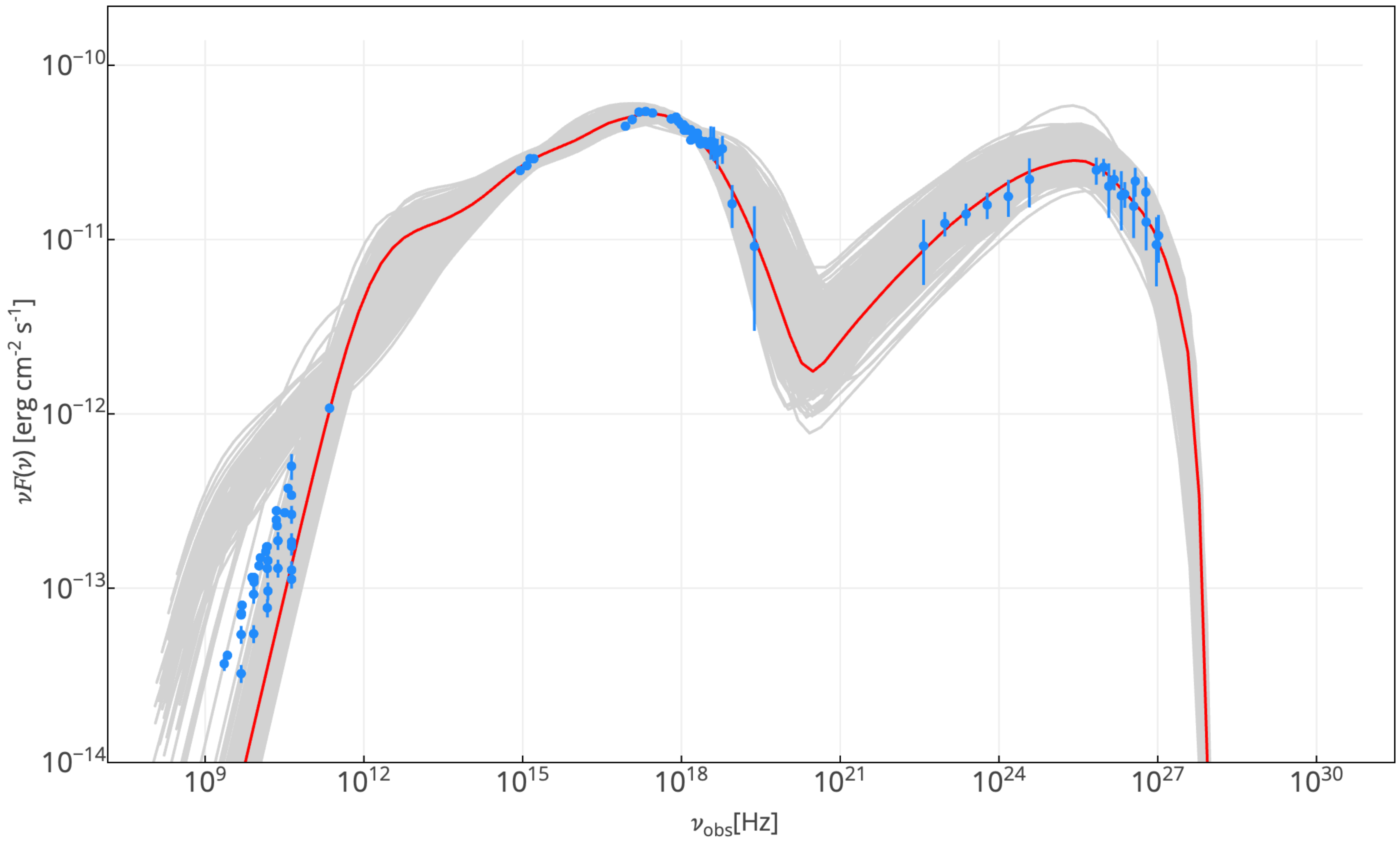

SSC EIC

Hadronic

p: 2.587

δ: 28.662

log10(γmin): 3.266

log10(γmax): 6.594

log10(B/[G]): -2.760

log10(R/[cm]): 17.518

log10(Le/[erg s^{-1}]): 44.629

z: 0.034

EBL

RUN MODEL

Conclusions

- ☑ Astrophysical data in the 1970s were sent by post on magnetic tape.
- ☑ There is now exponential growth in astronomical data volumes, driven by advancements in observational technologies and an increasing number of telescopes observing in different bands.
- ☑ AI and ML have revolutionized our approach to studying the universe, aiming to uncover hidden characteristics within data, enabling faster simulations, improved observations, and deeper understandings of cosmic phenomena.
- ☑ Astrophysical research will largely benefit from new developments in AI/ML.